



## Article

# Recent Meta-Heuristic Algorithms with a Novel Premature Convergence Method for Determining the Parameters of PV Cells and Modules

Mohamed Abdel-Basset <sup>1</sup>, Reda Mohamed <sup>1</sup>, Mohamed Abouhawwash <sup>2,3,\*</sup> , Yunyoung Nam <sup>4,\*</sup>  and Attia El-Fergany <sup>5</sup>

<sup>1</sup> Department of Computer Science, Faculty of Computers and Informatics, Zagazig University, Zagazig 44519, Egypt; mohamedbasset@zu.edu.eg (M.A.-B.); redamoh@zu.edu.eg (R.M.)

<sup>2</sup> Department of Mathematics, Faculty of Science, Mansoura University, Mansoura 35516, Egypt

<sup>3</sup> Department of Computational Mathematics, Science, and Engineering (CMSE), College of Engineering, Michigan State University, East Lansing, MI 48824, USA

<sup>4</sup> Department of Computer Science and Engineering, Soonchunhyang University, Asan 31538, Korea

<sup>5</sup> Electrical Power and Machines Department, Faculty of Engineering, Zagazig University, Zagazig 44519, Egypt; el-fergany@ieee.org

\* Correspondence: abouhaww@msu.edu (M.A.); ynam@sch.ac.kr (Y.N.)



check for updates

**Citation:** Abdel-Basset, M.; Mohamed, R.; Abouhawwash, M.; Nam, Y.; El-Fergany, A. Recent Meta-Heuristic Algorithms with a Novel Premature Convergence Method for Determining the Parameters of PV Cells and Modules. *Electronics* **2021**, *10*, 1846. <https://doi.org/10.3390/electronics10151846>

Academic Editor: Faranda Roberto Sebastiano

Received: 22 June 2021

Accepted: 28 July 2021

Published: 31 July 2021

**Publisher's Note:** MDPI stays neutral with regard to jurisdictional claims in published maps and institutional affiliations.



**Copyright:** © 2021 by the authors. Licensee MDPI, Basel, Switzerland. This article is an open access article distributed under the terms and conditions of the Creative Commons Attribution (CC BY) license (<https://creativecommons.org/licenses/by/4.0/>).

**Abstract:** Currently, the incorporation of solar panels in many applications is a booming trend, which necessitates accurate simulations and analysis of their performance under different operating conditions for further decision making. In this paper, various optimization algorithms are addressed comprehensively through a comparative study and further discussions for extracting the unknown parameters. Efficient use of the iterations within the optimization process may help meta-heuristic algorithms in accelerating convergence plus attaining better accuracy for the final outcome. In this paper, a method, namely, the premature convergence method (PCM), is proposed to boost the convergence of meta-heuristic algorithms with significant improvement in their accuracies. PCM is based on updating the current position around the best-so-far solution with two-step sizes: the first is based on the distance between two individuals selected randomly from the population to encourage the exploration capability, and the second is based on the distance between the current position and the best-so-far solution to promote exploitation. In addition, PCM uses a weight variable, known also as a controlling factor, as a trade-off between the two-step sizes. The proposed method is integrated with three well-known meta-heuristic algorithms to observe its efficacy for estimating efficiently and effectively the unknown parameters of the single diode model (SDM). In addition, an RTC France Si solar cell, and three PV modules, namely, Photowatt-PWP201, Ultra 85-P, and STM6-40/36, are investigated with the improved algorithms and selected standard approaches to compare their performances in estimating the unknown parameters for those different types of PV cells and modules. The experimental results point out the efficacy of the PCM in accelerating the convergence speed with improved final outcomes.

**Keywords:** PV systems; steady-state characterizations; optimization algorithms; premature convergence method

## 1. Introduction

Solar energy converted to electric power using a photovoltaic (PV) system offers considerable opportunities to overcome the drawbacks of the traditional energy sources in terms of unavailability, environmental pollution, and global warming [1–5]. Some of the advantages which show the importance of solar cells as mentioned in [6] are stated as follows:

- Less operational cost [7];

- Low maintenance [8];
- Reducing air population [9].

Solar energy also varies daily and is affected by transient obstructions due to cloud cover; thus, there is an essential need to optimize the performance of the PV system to reach the best output, especially under irradiance and temperature variation. Simulation, evaluation, and control of PV systems require an accurate model that accurately represents the nonlinear current-voltage (I-V) characteristics curve of the PV cells. Consequently, over the last decades, several different models have been proposed for simulating this curve [10].

Based on the PV model, analytical, deterministic, and meta-heuristic methods have been proposed to estimate the unidentified parameters of the three principal types of PV models, namely, single diode model (SDM), double diode model (DDM), and triple diode model (TDM), to improve the performance of the PV system. Analytical methods are based on the solution of a series of mathematical equations and have the advantages of ease of implementation and speed. However, there is not a sufficient match between the simulated and measured I-V curves [11,12]. Deterministic methods have constraints on the model, such as convexity and differentiability, depend heavily on the initial guess, and are easily trapped in local minima [13]. PV models are often implicit, multimodal, and nonlinear, which means that they are poorly solved using deterministic methods, such as Lambert W-functions [14], iterative approach [15], and the Newton–Raphson method [12,16].

Meta-heuristic algorithms have been shown to overcome several real-world problems in a reasonable time with high accuracy [17–22] and therefore have been widely applied for tackling the parameter identification problem (PIP) of PV models. This section reviews the major applications and their shortfalls.

Xiong et al. [23] proposed the competitive swarm optimization (CSO) approach based on an advanced variant of particle swarm optimization (PSO) for identifying the unidentified parameters of the PV models. However, the authors found that this advanced variant of PSO still suffers from falling into local minima for complex multimodal optimization problems such as the PIP of PV models because of its weak exploration capability. Therefore, CSO was improved by two strategies to improve its exploration capability. The first was the winner-leading search strategy proposed to make the losers explore more regions within the search space. The second strategy is the Gaussian mutation operator that was proposed to improve the exploration operator of CSO to escape the local minima problem. The resultant version of CSO integrated with the winner-leading search and the Gaussian mutation was called WLCSDGM and was extensively investigated on four PV models and compared with 12 optimization algorithms to check its superiority.

Diab et al. [24] proposed the coyote optimization algorithms (COA) for tackling the PIP of SDM, DDM, and TDM and was observed on multi-crystalline, mono-crystalline, and thin-film PV modules under various irradiance and temperature levels. Long et al. [10] integrated both the grey wolf optimizer and cuckoo search (CS) algorithm (GWOCS) for identifying the parameters of DDM, SDM, and PV modules based on the test points measured under various operation conditions. For increasing the diversity among the members of the GWO, the opposition learning strategy was integrated to balance the exploration and exploitation operators of GWOCS while avoiding local minima and moving accurately and quickly toward the optimal solution. To validate the performance of GWOCS, ten complex mathematical functions were investigated, in addition to estimating the parameters of the different PV models as a harder problem with several local minima.

Ridha et al. [25] proposed the boosted Harris hawks optimization algorithm (BHHO) for estimating the parameters of the solar cell SDM by taking into consideration the sensitivity under various sunlight and temperature conditions. BHHO was enhanced by renting the exploration operator of the flower pollination algorithm and the vigorous mutation scheme of the DE to move quickly the individuals in a direction of the optimal solution and explore extensively the search space of the problem to find the most promising regions. The experimental outcomes show that BHHO is superior to some of the well-

known meta-heuristic optimization algorithms. Ultimately, Table 1 provides a brief review of some of the optimization algorithms proposed in the last two years for the SDM, DDM, and TDM PV models.

**Table 1.** Reviews of some studied algorithms for the PIP of different PV models.

Algorithm and Year	Contributions and Limitations
Classified Perturbation Mutation Based PSO Algorithm (CPMPSO, 2020) [11]	This algorithm divided the individuals into two categories according to the fitness values: The first one has individuals with high quality and is updated using an effective exploitation operator, while in the other, individuals had been updated using an effective exploration operator. Its convergence speed still needs improvement. Additionally, it has difficulty in avoiding becoming trapped in local minima for DDM.
Enhanced Adaptive Differential Evolution (EJADE, 2020) [12]	This algorithm used a number of improvements, namely, a crossover sorting mechanism for using the best individuals in the next generation to reach better outcomes, and a dynamic population reduction strategy to increase the convergence speed.
Whale Optimization Algorithm (WOA) based Reflecting Learning (RLWOA, 2020) [26]	WOA was improved using the reflection learning strategy to reduce the probability of becoming trapped in local minima, and subsequently increasing the possibility of reaching better outcomes. However, the increased speed of this algorithm against the studied algorithms was not analyzed.
Improved Equilibrium Optimizer (IEO, 2020) [27]	In this paper, EO was improved using two strategies: the first worked on accelerating the convergence, while the second was used to avoid becoming trapped into local minima. This algorithm produced good outcomes compared to four compared algorithms on three different PV models.
Improved Electromagnetism-like (IEM, 2020) [28]	A nonlinear equation was used to adjust the number of individuals in each generation to increase the convergence speed. Simplifying the total force formula to increase the exploration operator to explore the most promising regions for avoiding becoming stuck in local minima problems. Only validated on SDM, its performance is not known for DDM and TDM.
Flower Pollination Algorithm (FPA, 2020) [29]	The authors adapted FPA for estimating the parameters of DDM and used RTC France to validate its performance. Additionally, for verifying its performance, it was extensively compared with four studied algorithms. Unknown performance was compared with some of the recent robust algorithms published within the last two years.
Camel Behavior Search Algorithm (CBSA, 2020) [30]	For estimating the parameters of SDM for the multi-crystalline KC 200GT PV module, CBSA was proposed. This algorithm was validated on the SDM of the PV solar module, but its final outcome and convergence speed still need significant improvement.
Improved Social Spider Algorithm (ISSA, 2020) [31]	In this research, the social spider algorithm was proposed with an improvement in its performance to increase its exploration operator; this improvement was based on replacing the worst individuals within the populations with other solutions within the search space of the problem after a period of the iteration.
A hybrid WOA and PSO Algorithm (HWOA, 2021) [32]	In this paper, a new parameter estimation algorithm based on integrating PSO with WOA and a pipeline model was proposed to accurately speed the convergence rate. The experimental outcomes affirm that this algorithm was better than all the compared for the convergence rate and accuracy.
A Modified Whale Optimization Algorithm (MWOA, 2021) [33]	In this paper, MWOA was proposed to overcome stagnation into local minima, and low convergence speed by employing a mutation operator based on the levy flight, and a local search strategy to promote the exploitation capability. Thereafter, this algorithm was employed for tackling the parameter estimation of the PV models and could fulfill superior performance.
An enhanced JAYA (EJAYA, 2021) [34]	Recently, a new variant of the JAYA algorithm, namely, EJAYA, has been developed to improve the standard algorithm using three effective improvements. EJAYA could be the best solution, compared to some related techniques.
Enhanced Levy Flight Based Grasshopper Optimization Algorithm (LGOA, 2021) [35]	The levy flight was integrated into the grasshopper optimization algorithm to utilize its advantages in preserving the diversity among the populations in addition to enhancing the exploitation capability for proposing a new solar cell parameter estimation technique named LGOA.

Table 1. Cont.

Algorithm and Year	Contributions and Limitations
Gradient-Based Optimizer (GBO, 2021) [36]	To extract five, seven, and nine unknown parameters of SDM, DDM, and TDM, respectively, the gradient-based optimizer was recently proposed for tackling the global optimization problem, for which it was adapted due to having a high convergence speed with a highly local minima avoidance strategy. The experimental outcomes show the proficiency of this developed algorithm.
Harris Hawks Optimization Algorithm (HHO, 2020) [37]	The application of HHO to estimate the unknown parameters of the PV models has been recently proposed to examine its efficiency in comparison to some of the other optimization algorithms. The experimental findings show the efficiency of HHO over the compared ones.

From the preceding review, it is clear that most of the algorithms suffer from low convergence speed, consuming a large number of iterations without any great benefit. Therefore, in this paper, a new method called the premature convergence method (PCM) has been proposed to help the optimization algorithms in utilizing the iterations as much as possible to accelerate convergence and achieve better accuracy. PCM is based on a controlling factor used to determine if the current particle will be updated around the best-so-far solution in the direction of one of the following:

- (a) Two solutions selected randomly from the population;
- (b) The current position and the best-so-far solution;
- (c) Balancing between the previous two steps.

PCM is integrated with three well-known meta-heuristic algorithms: Harris hawks optimization [38], moth–flame optimizer [39], and equilibrium optimizer (EO) [40] to identify its efficacy for estimating the parameter of the SDM. The three algorithms were here used because they have a high exploration rate at the beginning of the optimization process that may lead to the consumption of a large number of iterations without reaching better outcomes to accelerate convergence in a direction of the optimal solution. Moreover, the search direction of these algorithms is not based on the direction in which the current population move, and that may make the algorithms search randomly for better outcomes in the exploration case or move in the same direction of the best-so-far solution that may promote falling into local minima in the exploitation case.

A PV cell based on the RTC France and three PV modules (Photowatt-PWP201, STM6-40/36, and Ulta 85-P) were used to investigate the performance of the PCM-improved versions of each algorithm compared with the standard version. The experimental results show the effectiveness of the integration of PCM with each of the three optimization algorithms, particularly with EO.

The remainder of this paper is organized as follows: Section 2 describes the SDM and PV module model. Furthermore, Section 3 describes the meta-heuristic algorithms and the premature convergence method. Section 4 gives the experimental results of the studied algorithms in addition to some discussions on those results. Finally, Section 5 provides conclusions and some discussion on future work.

## 2. Mathematical Descriptions of the Problem

This section described in detail the mathematical model of the single diode model and the PV module model, in addition to the objective function used in this work.

### 2.1. Single Diode Model (SDM)

As illustrated in Figure 1, the SDM is simple, comprising the photo-generated current  $I_{ph}$  [41], the diode current as estimated using Equation (1), the shunt resistor current as calculated according to Equation (3), and  $I$  that indicates the output current of the SDM.

$$I_D = I_{sd} \left( \exp \left( \frac{V + I \times R_s}{n \times V_t} \right) - 1 \right) \quad (1)$$



where  $I_{sd}$  is the diode current,  $V$  indicates the output voltage,  $R_s$  is the series resistance,  $n$  is the ideality factor of the diode, and  $V_t$  is the junction thermal voltage and mathematically formulated as

$$V_t = \frac{k \times T}{q} \tag{2}$$

$T$  is the temperature of the junction in kelvin,  $k$  is the Boltzmann constant ( $1.3806503 \times 10^{-23}$  J/K), and  $q$  refers to the electron charge ( $1.60217646 \times 10^{-19}$  C).

$$I_{sh} = \frac{V + I \times R_s}{R_{sh}} \tag{3}$$

$R_{sh}$  is the shunt resistance. By replacing  $I_D$  and  $I_{sh}$  in Equation (4) with their formula defined in Equations (1) and (3),  $I$  is as follows:

$$I = I_{ph} - I_D - I_{sh} \tag{4}$$

$$I = I_{ph} - I_{sd} \left( \exp \left( \frac{q * (V + I \times R_s)}{n \times k \times T} \right) - 1 \right) - \frac{V + I \times R_s}{R_{sh}} \tag{5}$$

For the SDM, five known parameters ( $I_{ph}$ ,  $I_{sd}$ ,  $n$ ,  $R_s$ ,  $R_{sh}$ ) therefore need to be estimated efficiently to optimize the performance of the PV system.

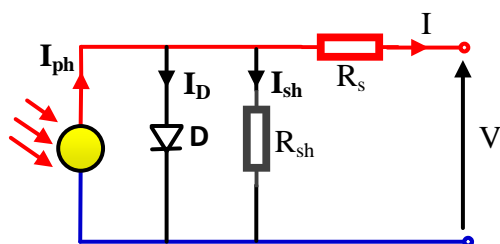


Figure 1. Equivalent circuit of SDM.

### 2.2. Photovoltaic (PV) Module Model

The PV cell produces extremely small amounts of useful electricity on its own, and therefore,  $N_s$  PV cells are connected in series to form a practical solar cell unit known as a PV module to supply the required output current and power. The PV module can be formulated as Equation (5) with the difference that  $V_t$  is computed as follows:  $V_t = (N_s kT)/q$  [42].

For the nonstandard conditions unlike STC, the above-stated mathematical model should be altered to show the performances under varied cell temperatures and changed radiation levels. The equation’s model should be adapted to accommodate such changes due to  $G$  and  $T$  variations as follows [6,35–37,43,44]:

$$I_{ph} = \frac{G}{G^{STC}} \left[ I_{ph}^{STC} + K_i(T - 25) \right] \tag{6}$$

$$V_{oc} = V_{oc}^{STC} + K_v(T - 25) \tag{7}$$

$$E_g = E_g^{STC} \left[ 1 - 2.677 \times 10^{-4}(T - 25) \right] \tag{8}$$

$$I_{sdi} = I_{sdi}^{STC} \left( \frac{T}{25} \right)^3 \cdot \exp \left( \frac{q \cdot E_g(T - 25)}{25 a_i \cdot K \cdot T} \right), \forall i \in 1 : 3 \tag{9}$$

$$R_{sh} = R_{sh}^{STC} \cdot \left( \frac{G^{STC}}{G} \right) \tag{10}$$

where  $K_i$  and  $K_v$  define the thermal coefficient of current and voltage, respectively,  $E_g$  denotes the semiconductor band-energy,  $V_{oc}$  denotes open-circuited voltage, and others are the normalized parameters at STC.

### 3. Meta-Heuristic Algorithms and the Premature Convergence Method

The meta-heuristic algorithms have sought to find the near-optimal solutions of the optimization problem based on two operators—exploration and exploitation. In the exploration operator, the algorithm explores most regions of the search space searching extensively for the promising region that may significantly contain the optimal solution. Then, within the first half of the optimization process, the exploitation operator may be applied to search around the current promising region for better solutions. In the second half of the optimization process, the exploitation is mandatorily applied as an attempt to exploit the last current promising region that may contain the global solution.

In this section, three optimization algorithms are described, in addition to the PCM. First, before describing each algorithm separately, it is useful to explain the stage shared between them—the initialization step. In the initialization step, a population with  $N$  individuals of  $d$  dimensions, where  $d$  is the number of the unknown parameters in the problem, are distributed within the search space of the problem using Equation (11) as the start point upon which the optimization process relies.

$$\vec{X}_i = \vec{L}_{min} + \left( \vec{U}_{max} - \vec{L}_{min} \right) \times \vec{r}, \forall i \in N \quad (11)$$

where  $\vec{X}_i$  is a vector to load the position of the  $i$ th individual,  $r$  is a vector generated randomly at the range of 0 and 1, and  $\vec{L}_{min}$  and  $\vec{U}_{max}$  are two vectors, including the lower bound and upper bound of each unknown parameter in the solved problem.

#### 3.1. Objective Function

The root mean squared error (RMSE) between the measured and estimated current that is computed under the estimated parameters and the Newton–Raphson method [43] will be used as an objective function to evaluate the quality of each solution in the population. This objective function defined according to RMSE is formulated as

$$\text{RMSE} = f(\vec{X}_i) = \sqrt{\frac{1}{M} \times \sum_{k=1}^M (I_m - I_e)^2} \quad (12)$$

where  $I_m$  indicates the measured current,  $M$  is the number of the measured test points, and  $I_e$  is the simulated current and defined as

$$I_{k+1} = I_k - \frac{F(I)}{F'(I)} \quad (13)$$

$F(I)$  is computed according to Equation (5) and  $F'(I)$  is the first derivative of the same equation with respect to  $I$ . In common practice, five iterations are sufficient to solve the above, as stated in (13) with a very acceptable tolerance using the NR method.

#### 3.2. Premature Convergence Method (PCM)

In this section, a novel method known as a premature convergence method is proposed to help the optimization algorithm in accelerating the convergence speed with avoiding becoming trapped in local minima. This method also includes a control factor  $r$  generated randomly between 0 and 1. According to the control factor, the exploitation capability will be significantly encouraged when  $r > 0.5$ , while the exploration operator is applied to the current position if  $r < 0.5$ , and balancing between the exploration and exploitation

operators is achieved in a case of  $r = 0.5$ . Finally, each solution under the PCM will be updated according to the following equation:

$$\vec{nX}_i(it + 1) = \vec{X}^* + (1 - r) * \left( \vec{X}_a(it) - \vec{X}_b(t) \right) + (r) * \left( \vec{X}^* - \vec{X}_i(it) \right) \quad (14)$$

where  $a$  and  $b$  are two integers selected randomly between 1, and  $N$  and represent the indices of two individuals within the population.  $\vec{nX}_i$  is a vector used to store the next position of the  $i$ th individual, and  $\vec{X}^*$  is the best-so-far solution obtained by any optimization algorithm. Finally, the steps of this method are presented in Algorithm 1.

---

#### Algorithm 1 The steps of PCM

---

**Input:** current population  $\vec{X}_i, i = 1, 2, 3, 4, \dots, N$

1. **for** each  $i$  individual
2.     Update  $\vec{X}_i$  using Equation (14)
3.     **If**  $f(\vec{X}_i) > f(\vec{nX}_i)$
4.          $\vec{X}_i = \vec{nX}_i;$
5.     **end**
6. **end for**

**Output:** return  $\vec{X}$

---

After describing the main steps of PCM, in the next subsections, this method is integrated with three well-known optimization algorithms to identify its influence on the performance of those algorithms.

### 3.3. Meta-Heuristic Algorithms

#### 3.3.1. Equilibrium Optimizer

Recently, a novel physics-based optimization algorithm known as the equilibrium optimizer (EO) was proposed by Faramarzi [40] for solving global optimization problems. The mathematical model of EO is described in detail.

At the outset, the equilibrium state of the system is not known; thus, EO considers the best-so-far four particles, in addition to their average as the equilibrium candidates, and adds them in the ascending order according to their fitness values if the problem is minimized inside an equilibrium pool  $\vec{p}_{eq,pool}$ , as described in Equation (15); the first four particles encourage the exploration capability, while the last promotes the exploitation capability.

$$\vec{p}_{eq,pool} = \left[ \vec{X}_{eq(1)}, \vec{X}_{eq(2)}, \vec{X}_{eq(3)}, \vec{X}_{eq(4)}, \vec{X}_{eq(avg)} \right] \quad (15)$$

After defining the candidate solutions, the optimization process begins to update the individuals within the population by searching for other better solutions. EO seeks a reasonable balance between exploration and exploitation according to the following equation:

$$\vec{F} = a_1 \text{sign}(\vec{r} - 0.5) \left[ e^{-\vec{\lambda}(t)} - 1 \right] \quad (16)$$

$\lambda$  and  $r$  are two vectors containing values created randomly between 0 and 1, and  $t$  is computed as

$$t = \left( 1 - \frac{it}{t_{max}} \right)^{(a_2 * (\frac{it}{t_{max}}))} \quad (17)$$

where  $it$  indicates the current generation,  $t_{max}$  indicates the maximum of generations,  $a_2$  is a constant value to control the exploitation, and  $a_1$  is a constant value controlling the

diversification (exploration) capability. Another factor  $G$  represents the generation rate and is used to enhance the intensification/exploitation operator of EO,

$$\vec{G} = \vec{G}_0 * \vec{F} \quad (18)$$

$$\vec{G}_0 = \vec{GCP} * \left( \vec{X}_{eq} - \lambda * \vec{X} \right) \quad (19)$$

$$\vec{GCP} = \begin{cases} 0.5r_1 & r_2 > GP \\ 0 & otherwise \end{cases} \quad (20)$$

where  $r_1$  and  $r_2$  are numbers generated randomly within 0 and 1.  $GP$  is a constant parameter used to balance the ratio between diversification and intensification operators of EO. In the end, each individual within the population is generally updated as defined in Equation (21).

$$\vec{X} = \vec{X}_{eq} + \left( \vec{X} - \vec{X}_{eq} \right) * \vec{F} + \frac{\vec{R}}{\lambda * V} * \left( 1 - \vec{F} \right), V = 1 \quad (21)$$

Finally, the steps of EO integrated with the PCM are given in Algorithm 2 and Figure 2. Integrating PCM with EO helps to explore the promising regions obtained by it at each generation as an attempt to see if the near-optimal solution is there or not. If the optimal solution is found, that will reduce the number of function evaluations consumed by the standard algorithm even reaching or might the maximum evaluations is terminated without reaching this optimal solution. Therefore, we integrated this strategy to improve the exploitation capability of the meta-heuristic algorithms, which has a high-exploration operator at the beginning of the optimization process to avoid the initial time-consuming process by the standard algorithm in its search for the promising region; this solution already emerged in the previous generation and need only to be more focused for achieving the near-optimal solution.

### 3.3.2. Moth–Flame Optimizer

Mirjalili [39] proposed a novel meta-heuristic algorithm, called the moth–flame optimization algorithm (MFO), based on the navigation strategy of the moths in nature. According to [39], the MFO algorithm consists of three phases: initialization phase, updating phase, and stopping conditions. After distributing  $N$  moths within the search space of the problem using Equation (11), the fitness value for each is computed, and the best positions of the moths will be assigned to flames. Then, the optimization process will update the positions of moths based on the flames as defined in the following equation:

$$X_i = F_j + D_i e^{bl} \cos(2\pi l), i, j = 1, 2, 3, \dots, N \quad (22)$$

$$D_i = |F_j - X_i| \quad (23)$$

where  $l$  is a random number between 1 and  $-1$ , and  $b$  refers to the  $j$ th flame that is used to define the shape of the logarithmic spiral function. To avoid degrading the exploitation of the best solution, the number of flames (`flame_no`) must be decreased according to the adaptive mechanism strategy defined in Equation (24) to make the algorithm focus on the best-so-far solution in a hope of finding a better solution.

$$flame\_no = round\left(N - it \times \frac{N - 1}{t_{max}}\right) \quad (24)$$

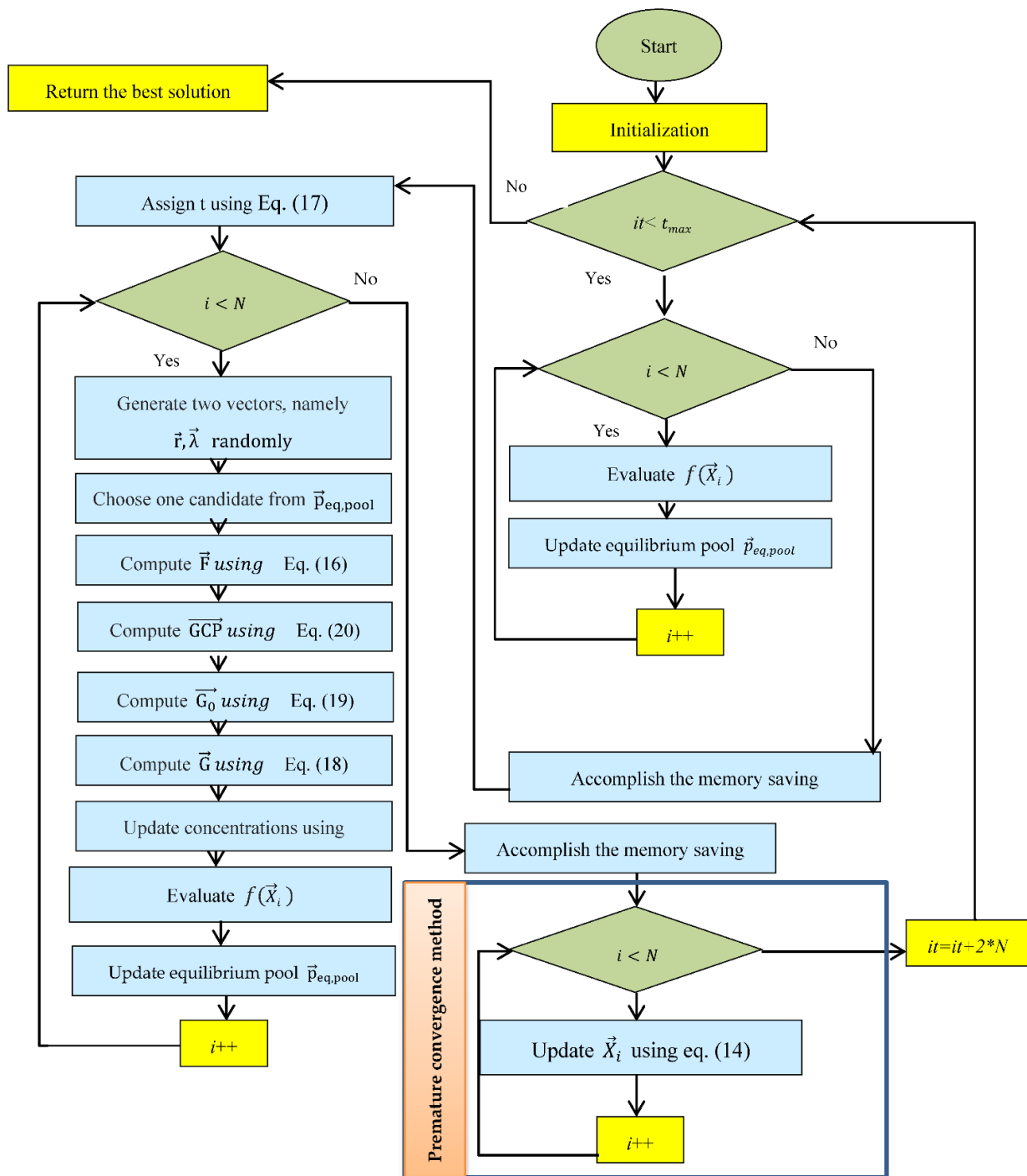


Figure 2. Flowchart of hybridization between PCM and EO.





**Algorithm 3** The steps of PCM integrated MFO(PMFO)

1. Initialization step
2.  $MF_1$  = Calculate  $f(\vec{X}_i)$  for each moth.
3.  $it = 1$
4. **while** ( $it < t_{max}$ )
5.     Update  $flame\_no$  using Equation (24)
6.     **if**  $it==1$
7.          $F$  = sort  $\vec{X}$  according to  $MF_1$ ;
8.          $FF$  = sort( $MF_1$ ); //sort the fitness values of moths
9.     **Else**
10.          $MF_{it}$  = Calculate  $f(\vec{X}_i)$  for each moth.
11.          $F$  = sort ( $\vec{X}$  (it-1),  $\vec{X}$  (it)) according to their fitness values found in  $MF_{it-1}$  and  $MF_{it}$
12.          $FF$  = sort( $MF_{it-1}$ ,  $MF_{it}$ );
13.     **end**
14.     **for each**  $\vec{X}_i, i = 1, 2, 3, \dots, N$
15.         **If**  $i \leq flame\_no$
16.             Update  $\vec{X}_i$  according to equation (22) with respect to its corresponding flame.
17.         **else**
18.             Update  $\vec{X}_i$  according to Equation (22) with respect to the flame  $flame\_no$ .
19.         **End if**
20.          $it++$
21.     **end for**
22.     Update the current population using Algorithm 1.
23.      $it = it + N$
24. **end while**

3.3.3. Harris Hawks Optimization Algorithm

Haidari et al. [38] proposed a meta-heuristic algorithm inspired by the chasing style and cooperative behaviors of Harris hawks, known as the HHO algorithm. The mathematical model of HHO simulates the behaviors of the hawks where several hawks cooperatively swoop on prey, often a rabbit, from different paths to surprise it. Additionally, Harris hawks have the ability to reveal different types of chasing patterns to choose the best one according to the distinct patterns of prey flight. In the exploration phase, HHO enables a trade-off between updating the Harris hawk’s perch randomly at a location near other members and wait to find prey, and perch on random tall trees with an equal probability of  $q$  as follows:

$$\vec{X}(it + 1) = \begin{cases} \vec{X}_r(it) - r_1 \left| \vec{X}_r(it) - 2r_2\vec{X}(it) \right| & q \geq 0.5 \\ \vec{X}^*(it) - \vec{X}_{mean}(it) - r_3 \left( \vec{L}_{min} + r_4 \left( \vec{U}_{max} - \vec{L}_{min} \right) \right) & q < 0.5 \end{cases} \quad (25)$$

where  $\vec{X}(it)$  and  $\vec{X}(it + 1)$  are two vectors including the current and the next position of the hawks.  $\vec{X}_r(it)$  is a hawk selected randomly from the population.  $X^*(it)$  is the location of the rabbit, which is also called the best-so-far solution.  $q, r_1, r_2, r_3,$  and  $r_4$  are five numerical values generated randomly.  $\vec{X}_{mean}(it)$  indicates the mean position of solutions in the current population and computed as follows:

$$\vec{X}_{mean}(it) = \frac{1}{N} \sum_{i=1}^N \vec{X}_i(it) \quad (26)$$

According to the escaping energy  $E$  of the rabbit, HHO can move from the exploration to the exploitation operator as defined in the following equation:

$$E = 2E_0 \left( 1 - \frac{it}{t_{max}} \right) \tag{27}$$

where  $E_0$  indicates the initial energy of the rabbit and is generated randomly between  $-1$  and  $1$ . If  $|E| \geq 1$ , hawks explore more regions to search for the rabbit position, otherwise it will exploit the current rabbit location. Based on the value of  $E$ , the hawks will create their step sizes according to a soft ( $|E| \geq 0.5$ ) or hard ( $|E| < 0.5$ ) besiege. The soft besiege can be modeled as

$$\vec{X}(it + 1) = \vec{\Delta X}(it) - E \left| J\vec{X}^*(it) - \vec{X}(it) \right| \tag{28}$$

$$\vec{\Delta X}(it) = \vec{X}^*(it) - \vec{X}(it) \tag{29}$$

$$J = 2(1 - rand) \tag{30}$$

$J$  indicates the random jump strength of the rabbit;  $rand$  is a random number generated between  $0$  and  $1$ . The hard besiege can be mathematically formulated as follows:

$$\vec{X}(it + 1) = \vec{X}^*(it) - E \left| \vec{\Delta X}(it) \right| \tag{31}$$

where ( $|E| \geq 0.5$ ) and ( $p \geq 0.5$ ) in which the rabbit has enough energy to escape of the hawks, the soft besiege with progressive rapid dives (PRD) will be performed. Based on the actual behaviors of the hawks, they can choose the best possible dive toward the intended prey. In addition, in this phase, Lévy flight is used to mimic the escaping steps of the prey and the leapfrog of hawks. In this stage, the next position of the hawks is updated according to the following equation:

$$\vec{k} = \vec{X}^*(it) - E \left| J\vec{X}^*(it) - \vec{X}(it) \right| \tag{32}$$

If this updated position represented in  $k$  is not better than the current position represented  $X(it + 1)$ , the hawks will dive according to the Lévy flight  $L$  as follows [38]:

$$\vec{z} = \vec{k} + \vec{S} \times L(d) \tag{33}$$

$S$  is a numerical vector including random numbers. The final soft besiege can be summarized as

$$\vec{X}(it + 1) = \begin{cases} \vec{k} & \text{if } f(\vec{k}) < f(\vec{X}(it)) \\ \vec{z} & \text{if } f(\vec{z}) < f(\vec{X}(it)) \end{cases} \tag{34}$$

In the hard besiege with PRD, the rabbit has too low energy to run away from hawks, when ( $|E| < 0.5$ ) and ( $p < 0.5$ ) by using Equation (34) where  $Z$  is computed based on Equation (33) and  $k$  is updated according to the following:

$$\vec{X} = \vec{X}^*(it) - E \left| J\vec{X}^*(it) - \vec{X}_{mean}(it) \right| \tag{35}$$

Finally, the pseudo-code of the HHO hybridized with PCM is given in Algorithm 4. As in the EO and MFO, the HHO has a weak exploitation operator; therefore, due to the advantages of the PCM mentioned before, it is integrated with this algorithm to enhance

its exploitation operator for attacking the promising regions obtained in each generation as an attempt to find the near-optimal solution without consuming several iterations.

---

**Algorithm 4** The standard HHO algorithm with PCM (PHHO)

---

```

1. Initialization step.
2. Evaluate each hawk
3.  $\vec{X}^*$  = best-so-far hawk
4.  $it = 1$ 
5. while ( $it \leq t_{max}$ )
6.     compute E according to Equation (27)
7.     if ( $|E| \geq 1$ )
8.         Update  $X(it + 1)$  using Equation (25)
9.     end if
10.    if ( $|E| < 1$ )
11.        if ( $p \geq 0.5 \ \&\& \ |E| \geq 0.5$ )
12.            Reposition  $X(it + 1)$  based on soft besiege
13.        end if
14.        if ( $p \geq 0.5 \ \&\& \ |E| < 0.5$ )
15.            Reposition  $X(it + 1)$  based on hard besiege
16.        end if
17.        if ( $p < 0.5 \ \&\& \ |E| \geq 0.5$ )
18.            Reposition  $X(it + 1)$  based on soft besiege with PRD
19.        end if
20.        if ( $p < 0.5 \ \&\& \ |E| \geq 0.5$ )
21.            Reposition  $X(it + 1)$  based on hard besiege with PRD
22.        end if
23.    end if
24.    if ( $f(\vec{X}(t + 1)) < f(\vec{X}_{rabbit})$ )
25.        Update  $\vec{X}^* = X(it + 1)$ 
26.    end if
27.     $it = it + N$ 
28.    Update the current population using Algorithm 1.
29.    Update  $\vec{X}^*$  if there is better.
30.     $it = it + N$ 
31. end while
Output: return  $\vec{X}^*$ 

```

---

#### 4. Results and Discussion

In this section, the influence of the PCM is observed with three well-known optimization algorithms: EO, HHO, and MFO. To validate the algorithms, the study used a PV cell based on RTC France (RTC) in addition to STM6-40/36 (STM6) module, Photowatt-PWP201 (PWP201) module, and STP6-120/36 (STP6) module as three PV modules. To illustrate the efficacy of the algorithms, several statistical metrics were used: worst, best, Avg, standard deviation (SD), and rank. In addition, Boxplots were used to depict the four quartiles of the outcomes obtained. Further, the convergence speed of each improved algorithm using PCM was compared with the standard version. For each test case, various demonstrations of experimental versus model results are presented, along with principal characteristics under different operating conditions such as varying temperatures and sun irradiances.

The experiments were conducted on a device with RAM of 32 GB, Core (TM) i7, and Windows 10. MATLAB R2019a was used to implement the algorithms. In total, 30 independent runs were carried out to determine the stability of the algorithms.

##### 4.1. Datasets Description

The studied algorithms in this research were used to estimate the parameters of various photovoltaic (PV) models that include the SDM and PV models. For the RTC

France Si cell, the measured I-V data are estimated at irradiance level ( $G$ ) of  $1000 \text{ W/m}^2$  and temperature  $T = 33 \text{ }^\circ\text{C}$  [44]. On the other hand, for the PV modules, STM6, the PWP201, and Ultra 85-P modules are employed to validate the extracted parameters. The Photowatt-PWP201 module has  $N_s = 36$  cells connected in series and the measured I-V test points are measured at  $G = 1000 \text{ W/m}^2$  and  $T = 45 \text{ }^\circ\text{C}$  [44]. The mono-crystalline STM6 [45], and Ultra 85-P [46] modules consist of 36 monocrystalline PV cells connected in series and are measured under temperature levels of  $51 \text{ }^\circ\text{C}$ , and  $25 \text{ }^\circ\text{C}$ , respectively. The  $L_{min}$  and  $L_{max}$  of each known parameter according to the type of the PV cell and PV modules used in this study are given in Table 2, as described in the literature [13,16].

**Table 2.** The search boundaries of each unknown parameter.

Parameter	RTC		PWP201		STM6		Ultra 85-P	
	$L_{min}$	$L_{max}$	$L_{min}$	$L_{max}$	$L_{min}$	$L_{max}$	$L_{min}$	$L_{max}$
$I_{ph}$ (A)	0	1	0	2	0	2	4.9	5.73
$I_{sd}$ ( $\mu\text{A}$ )	0	1	0	50	0	50	$1.0 \times 10^{-3}$	0.5
$R_s$ ( $\Omega$ )	0	0.5	0	2	0	0.36	$1.0 \times 10^{-6}$	5
$R_{sh}$ ( $\Omega$ )	0	100	0	2000	0	1500	0.93	100
$n, n_1, n_2$	1	2	1	50	1	60	1.0	2.0

#### 4.2. Parameter Selection

All the algorithms were executed using an equal number of function evaluations and runs  $t_{max} = 50,000$  to make a fair comparison among the algorithms. Picking the best value for  $N$  may significantly affect the performance of the algorithm; thus, different values for this parameter are observed to determine the best value with each algorithm. After observing 5, 10, 15, 20, 25, 30, 35, 40, 45, 50, 55, 60, 65, 70, 75, and 80 for  $N$  and depicting the outcomes in Figure 3, it is obvious that the performance of MFO is extremely poor when  $N$  is 5, but for the higher values, the performance almost is competitive; therefore, we randomly selected a population size of 80 in the next experiments since the population size higher than 5 does not significantly affect its performance. The performance of PMFO with a population size higher than 35, according to Figure 3b, is approximately the same, and therefore, 35 was selected as a population size for this algorithm within the next experiments. The best value for the population size of the HHO, PHHO, EO, and PEO according to Figure 3c–f is, respectively, 80, 50, 40, and 30 because they are competitive with the other values. From Figure 3, it is also obvious that the performance of all algorithms is significantly degraded with the small population size up to 10. Therefore, it is recommended that the population size for those investigated algorithms be assigned a value higher than 10 to guarantee better performance.

#### 4.3. RTC France

In this section, the standard algorithms and the PCM-improved algorithms were investigated on the SDM for the RTC France solar cell. It is worth mentioning that the improved algorithms in the following tables start with the letter P to be distinguished from the standard. Table 3 shows the optimal parameters estimated by each algorithm with the corresponding RMSE. In addition, the entire Table 4 shows the values of the statistical measures obtained by each algorithm, and Figure 4 shows the convergence speed, both of which indicate that the improved version of each algorithm outperforms the standard version for the different statistical measures as well as convergence speed: MFO has an average fitness value of 0.0012948678, while PMFO has the lower average of 0.0007731606; HHO has an average of 0.0027623201, while PHHO has a better average higher convergence speed; EO has an average fitness value of 0.0007736621, while PEO has a significant improvement with a value of 0.0007730063 and with higher convergence rate. It is worth noting that PEO is the algorithm with the lowest RMSE and better convergence speed. Based on this result, it is concluded that the PCM has a significant



effect on the performance of the investigated meta-heuristic algorithms, and hence, this method considers a significant addition to the meta-heuristic algorithms for reaching better outcomes in less number function evaluations.

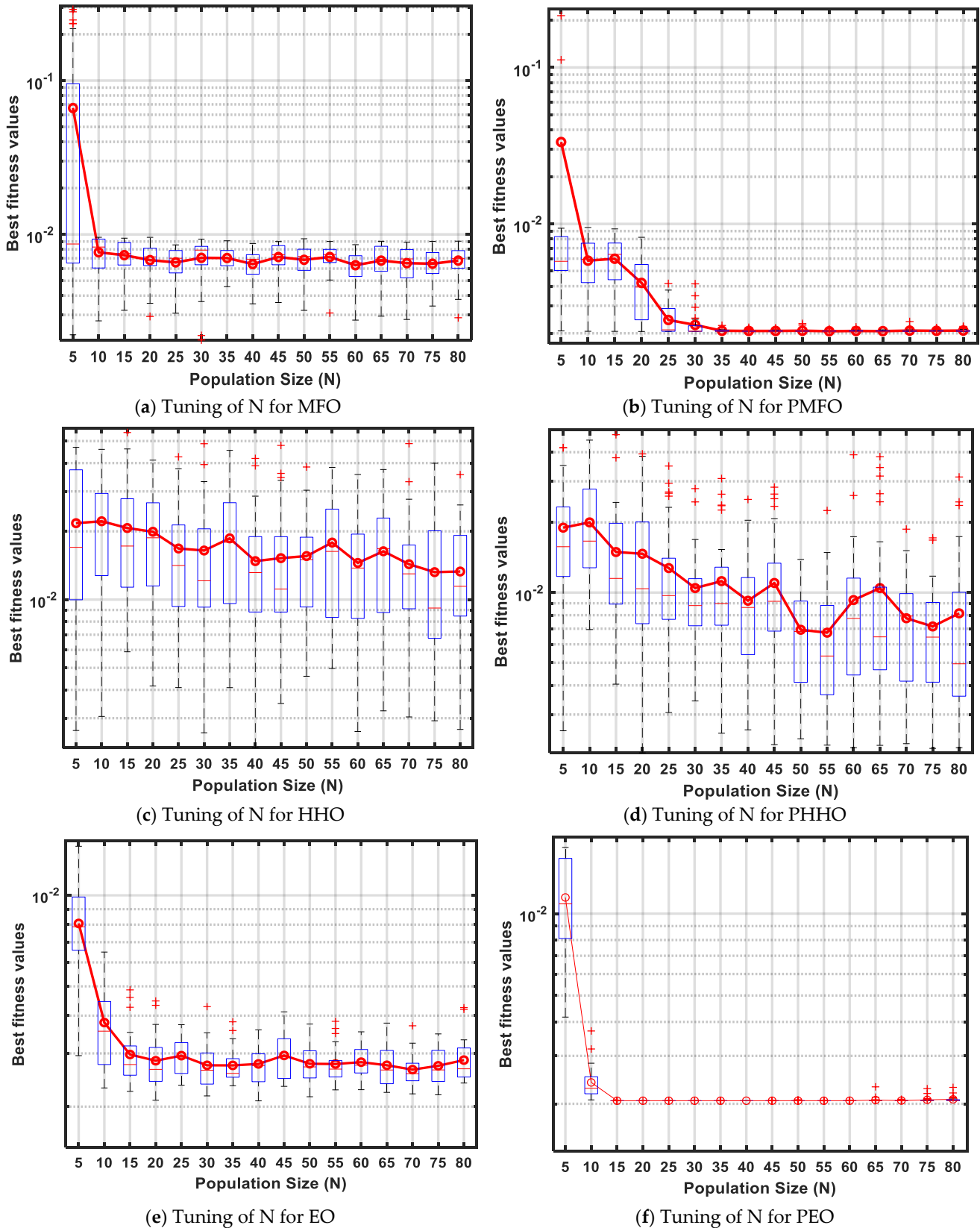


Figure 3. Tuning of N parameter.

**Table 3.** Comparison under the extracted parameters and the corresponding RMSE of RTC France.

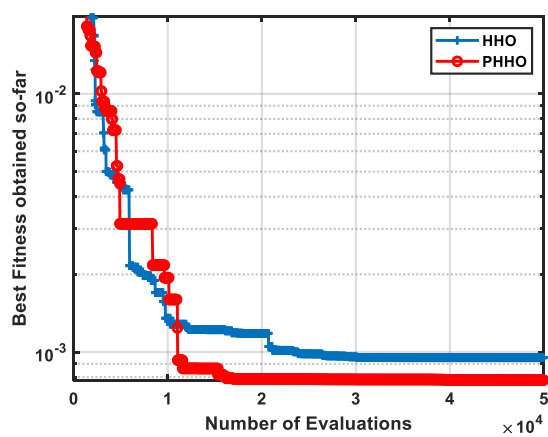
Algorithms	$I_{ph}(A)$	$I_d(A)$	$R_s(\Omega)$	$R_{sh}(\Omega)$	$n$	RMSE
MFO [39]	0.76062	$5.03 \times 10^{-7}$	0.03439	66.63760	1.52729	0.0007758336
PMFO	0.76070	$3.84 \times 10^{-7}$	0.03562	58.12059	1.49893	0.0007730647
HHO [38]	0.76235	$7.59 \times 10^{-7}$	0.03188	47.87549	1.57321	0.0007801742
PHHO	0.76643	$7.91 \times 10^{-7}$	0.03040	24.38538	1.57916	0.0008404323
EO [40]	0.75992	$4.48 \times 10^{-7}$	0.03513	80.93181	1.51476	0.0007731125
PEO	<b>0.76079</b>	<b><math>3.11 \times 10^{-7}</math></b>	<b>0.03655</b>	<b>52.88979</b>	<b>1.47727</b>	<b>0.0007730063</b>

Bold results are the best.

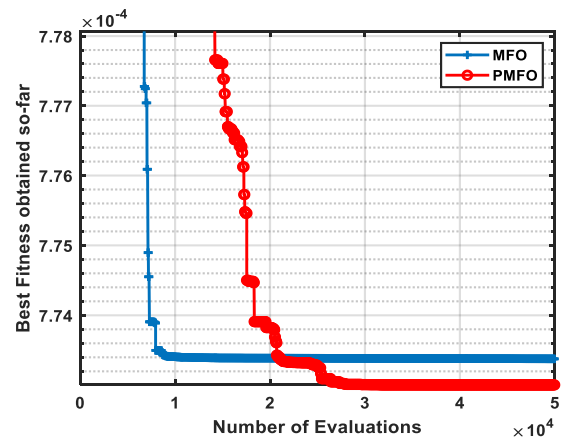
**Table 4.** Comparison of statistical measures of RTC France.

Algorithms	Best	Worst	Avg	SD	Rank
MFO [39]	0.0007787332	0.0023631263	0.0012948678	$4.2011 \times 10^{-4}$	4
PMFO	<b>0.0007730063</b>	0.0007762773	0.0007731606	$5.9821 \times 10^{-7}$	2
HHO [38]	0.0008065467	0.0072621800	0.0027623201	$1.7806 \times 10^{-3}$	6
PHHO	0.0007768550	0.0046230902	0.0014432096	$8.0094 \times 10^{-4}$	5
EO [40]	0.0007736621	0.0011382374	0.0008380151	$9.7150 \times 10^{-5}$	3
PEO	<b>0.0007730063</b>	<b>0.0007730063</b>	<b>0.0007730063</b>	<b><math>1.2633 \times 10^{-17}</math></b>	<b>1</b>

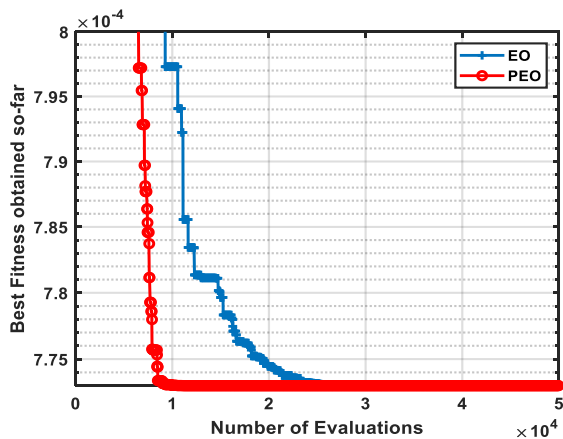
Bold results are the best option.



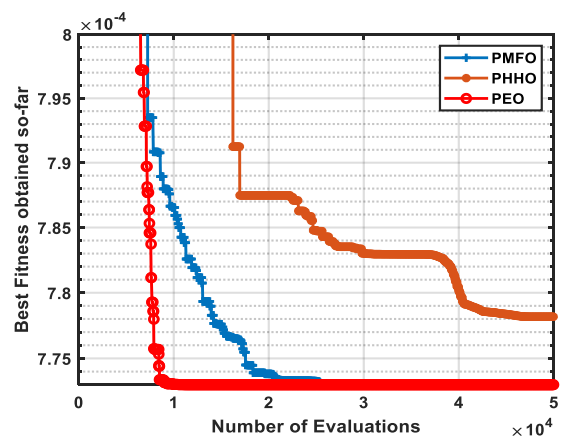
(a) HHO against PHHO



(b) MFO against PMFO



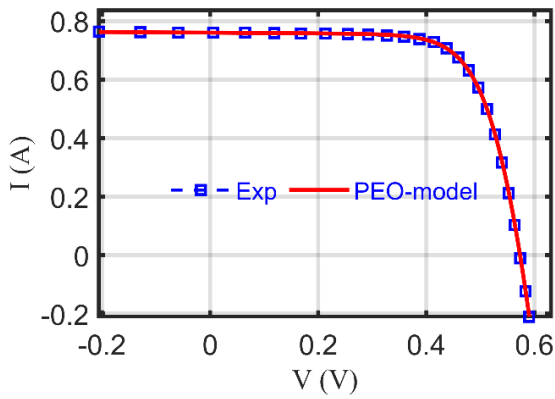
(c) EO against PEO



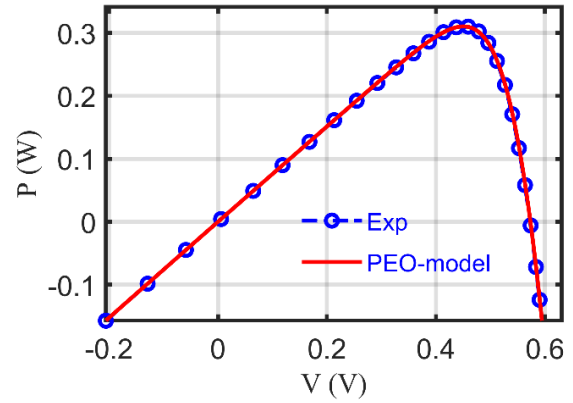
(d) PEO vs. PMFO vs. PHHO

**Figure 4.** Convergence curves among algorithms in RTC France.

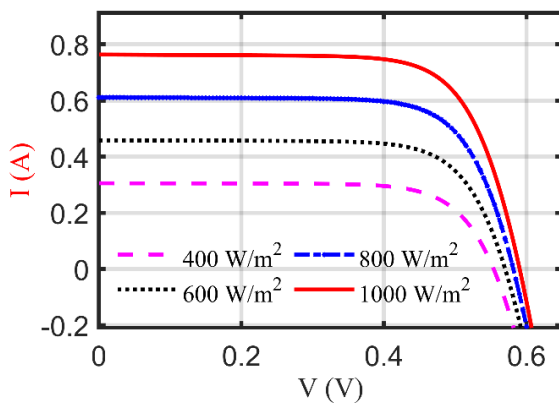
At this moment, various principal characteristics of this RTC Si PV cell can be generated using the cropped optimal values of the SDM parameters. Figure 5a,b illustrates the I–V and P–V plots of the PEO model against the real/experimental dataset points. On the other hand, various characteristics under varied sun irradiances (400–600–800–1000 W/m<sup>2</sup>) are revealed in Figure 5c,d, and under changeable cell, temperatures are shown in Figure 5e,f for 4 levels of temperatures at 0 °C to 75 °C in a step of 25 °C.



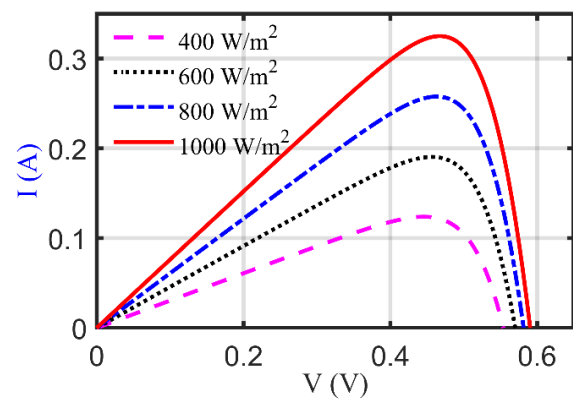
(a) I–V plots of experimental versus PEO model



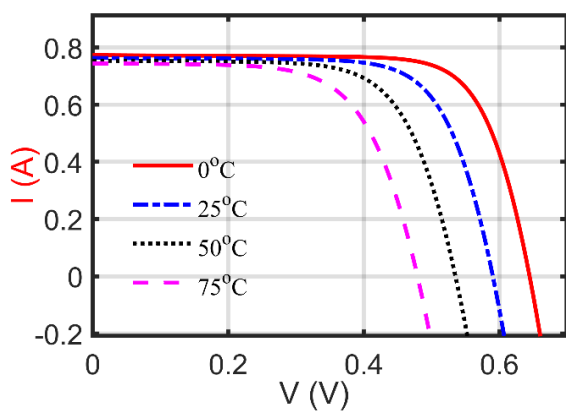
(b) P–V plots of experimental versus PEO model



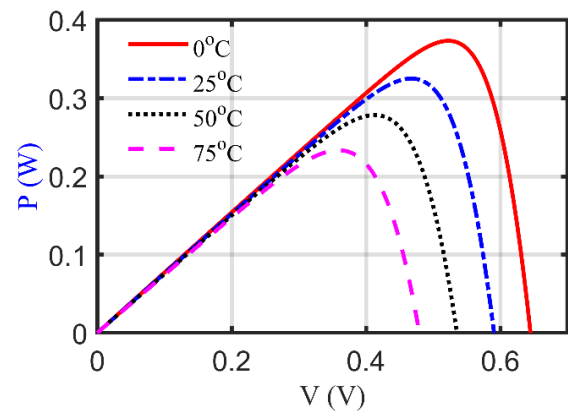
(c) I–V characteristics under different radiation levels



(d) P–V characteristics under different radiation levels



(e) I–V characteristics under varied temperatures



(f) P–V characteristics under varied temperatures

**Figure 5.** Principal characteristics of RTC France Si solar cell.

4.4. Photowatt-PWP201 Module

For this module, Table 5 presents the estimated parameters by each algorithm with the corresponding RMSE. Statistical measures are provided in Table 6, which shows that the performances of the algorithms integrated with PCM are significantly improved in terms of the final accuracy over the standard versions except for SCA that achieves a better outcome than the version integrated with PCM. The convergence speed of each standard algorithm against the improved version, in addition to the convergence speed among the improved versions, is given in Figure 6. From this figure, it can be inferred that PCM improved the classical algorithms for rapidly reaching better outcomes, compared to the classical ones, and consequently, this method is considered a good approach to overcome the convergence rate as the main shortcoming for most meta-heuristic algorithms. Again, this figure shows that PCM could accelerate the convergence speed of the classical EO in comparison to the other improved variants, as described also statistically in Table 5.

Table 5. Comparison under the extracted parameters per cell and the corresponding RMSE of Photowatt-PWP201.

Algorithms	Best	Worst	Avg	SD	Rank
MFO [39]	0.0021860541	0.0090007576	0.0064557976	$1.873147 \times 10^{-3}$	4
PMFO	<b>0.0020529606</b>	0.0022082698	0.0020813126	$4.057440 \times 10^{-5}$	2
HHO [38]	0.0042471828	0.0417859379	0.0177497759	$9.936836 \times 10^{-3}$	6
PHHO	0.0021488175	0.0267675029	0.0087683585	$5.384805 \times 10^{-3}$	5
EO [40]	0.0021180925	0.0036505619	0.0028887586	$4.197005 \times 10^{-4}$	3
PEO	<b>0.0020529606</b>	<b>0.0020529606</b>	<b>0.0020529606</b>	<b><math>2.3811 \times 10^{-17}</math></b>	1

Bold results are the best option.

Table 6. Comparison of statistical measures of Photowatt-PWP201.

Algorithms	$I_{ph}(A)$	$I_d(A)$	$R_s(\Omega)$	$R_{sh}(\Omega)$	$n$	RMSE
MFO [39]	1.03296	$1.82 \times 10^{-6}$	1.27671	656.49174	1.28548	0.0021860541
PMFO	1.03143	$2.64 \times 10^{-6}$	1.23563	821.64742	1.32217	0.0020529606
HHO [38]	1.03137	$1.09 \times 10^{-5}$	1.05025	1595.17923	1.48518	0.0042471828
PHHO	1.03027	$2.29 \times 10^{-6}$	1.25910	893.38027	1.30785	0.0021488175
EO [40]	1.02956	$3.23 \times 10^{-6}$	1.21509	1090.97355	1.34299	0.0021180925
PEO	<b>1.03143</b>	<b><math>2.64 \times 10^{-6}</math></b>	<b>1.23563</b>	<b>821.64129</b>	<b>1.32217</b>	<b>0.0020529606</b>

Bold results are the best option.

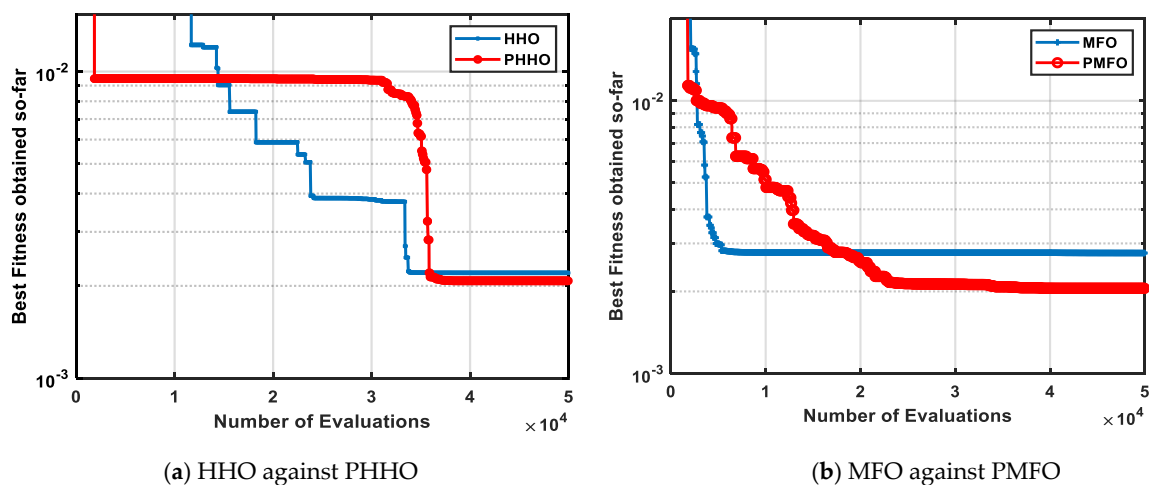


Figure 6. Cont.

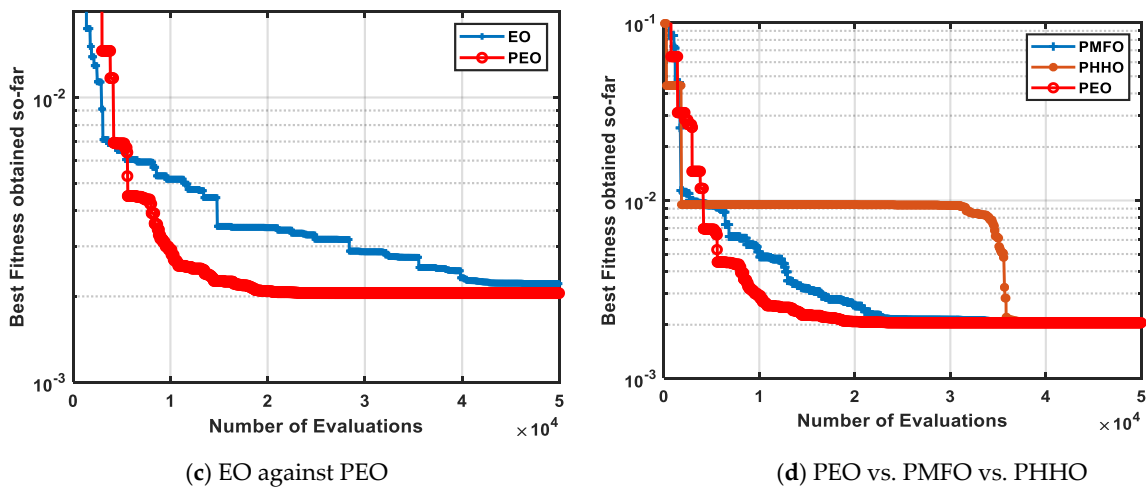
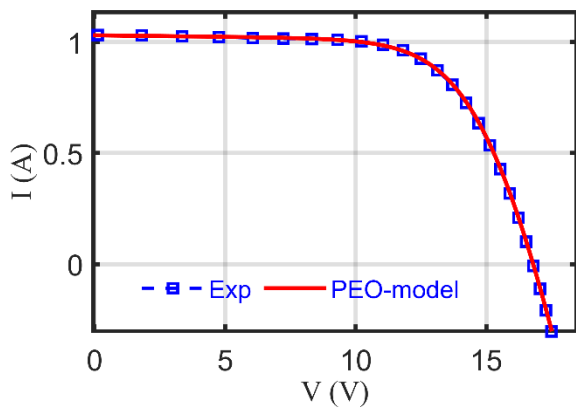
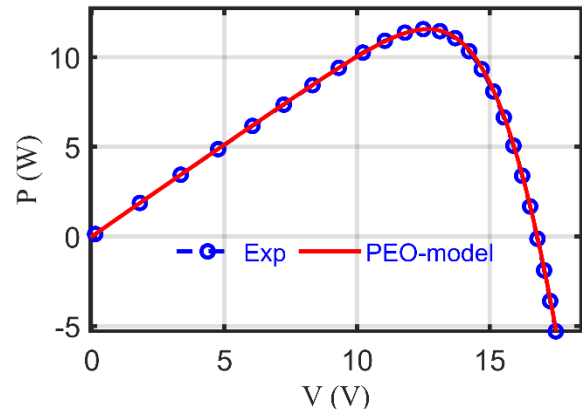


Figure 6. Convergence curves among algorithms in Photowatt-PWP201.

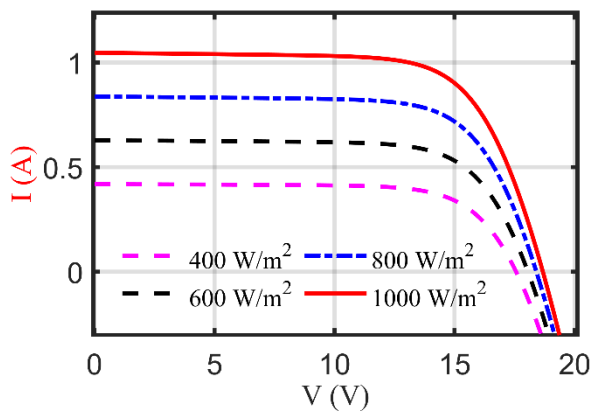
Once again, various principal characteristics of the PWP-201 module can be produced using the cropped optimal values of the SDM parameters. Figure 7a,b illustrates the I–V and P–V plots of the PEO model against the real/experimental dataset points. On the other hand, various characteristics under varied environmental conditions such as under varied sun irradiances (400–600–800–1000 W/m<sup>2</sup>) are revealed in Figure 7c,d, and under changeable cell, temperatures are shown in Figure 7e,f for 4 levels of temperatures at 0 °C to 75 °C in a step of 25 °C.



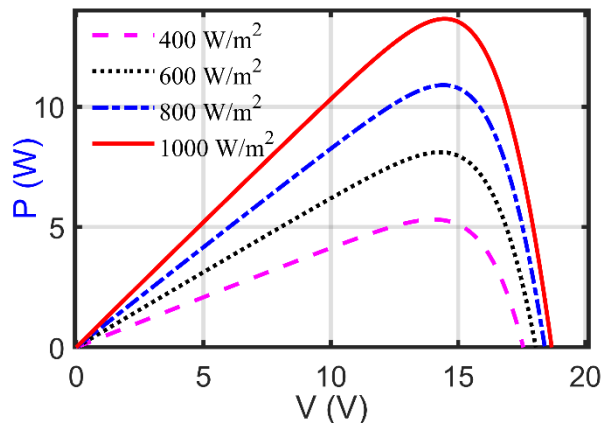
(a) I–V plots of experimental versus PEO model



(b) P–V plots of experimental versus PEO model



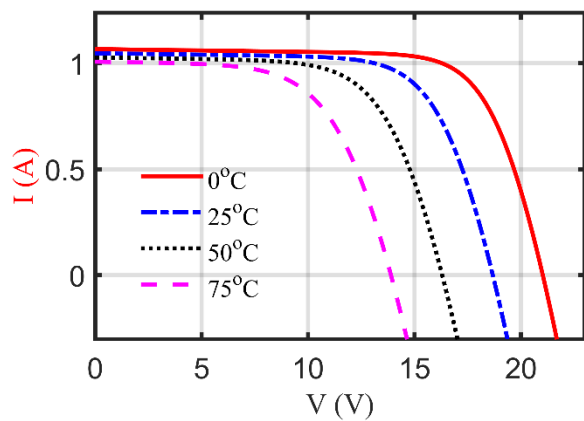
(c) I–V characteristics under different radiation levels



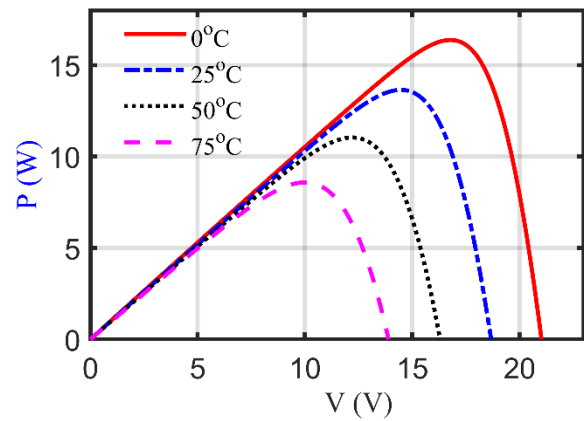
(d) P–V characteristics under different radiation levels

Figure 7. Cont.





(e) I–V characteristics under varied temperatures



(f) P–V characteristics under varied temperatures

Figure 7. Principal characteristics of PWP201 unit.

#### 4.5. STM6-40/36 Module

Each algorithm was executed 30 independent times and the optimal parameter values obtained through those runs were introduced in Table 7 with the corresponding RMSE. Table 8 shows the statistical measures for the best, SD, Avg, and worst obtained in those independent runs. This table confirms the superiority of the improved algorithm over the standard version for the three algorithms investigated. Figure 8 shows the better convergence of PMFO, PHHO, and PEO over the standard versions and also clarifies the competitiveness between PMFO and PEO.

Table 7. Comparison under the extracted parameters and the corresponding RMSE of STM6.

Algorithms	$I_{ph}(A)$	$I_d(A)$	$R_s(\Omega)$	$R_{sh}(\Omega)$	$n$	RMSE
MFO [39]	1.66229	$3.36 \times 10^{-6}$	0.07400	726.09128	1.59651	0.0023187518
PMFO	1.66391	$1.74 \times 10^{-6}$	0.15382	573.27439	1.52030	0.0017219251
HHO [38]	1.66127	$1.70 \times 10^{-6}$	0.18140	718.97910	1.51766	0.0026097874
PHHO	1.66691	$1.21 \times 10^{-6}$	0.18668	462.62209	1.48170	0.0021550622
EO [40]	1.66307	$2.11 \times 10^{-6}$	0.13187	624.29060	1.54203	0.0017870003
PEO	<b>1.66390</b>	<b><math>1.74 \times 10^{-6}</math></b>	<b>0.15364</b>	<b>573.53391</b>	<b>1.52047</b>	<b>0.0017219215</b>

Bold results are the best option.

Table 8. Comparison of statistical measures of STM6.

Algorithms	Best	Worst	Avg	SD	Rank
MFO [39]	0.0023187518	0.0225536598	0.0114708064	$6.7323 \times 10^{-3}$	5
PMFO	<b>0.0017219251</b>	0.0063436412	0.0021489829	$1.1362 \times 10^{-3}$	3
HHO [38]	0.0026097874	0.0613281613	0.0265107492	$1.6809 \times 10^{-2}$	6
PHHO	0.0021550622	0.0465598708	0.0107152318	$1.1196 \times 10^{-2}$	4
EO [40]	0.0017870003	0.0030841504	0.0024656101	$3.2718 \times 10^{-4}$	2
PEO	<b>0.0017219215</b>	<b>0.0017219215</b>	<b>0.0017219215</b>	<b><math>5.2394 \times 10^{-18}</math></b>	<b>1</b>

Bold results are the best option.

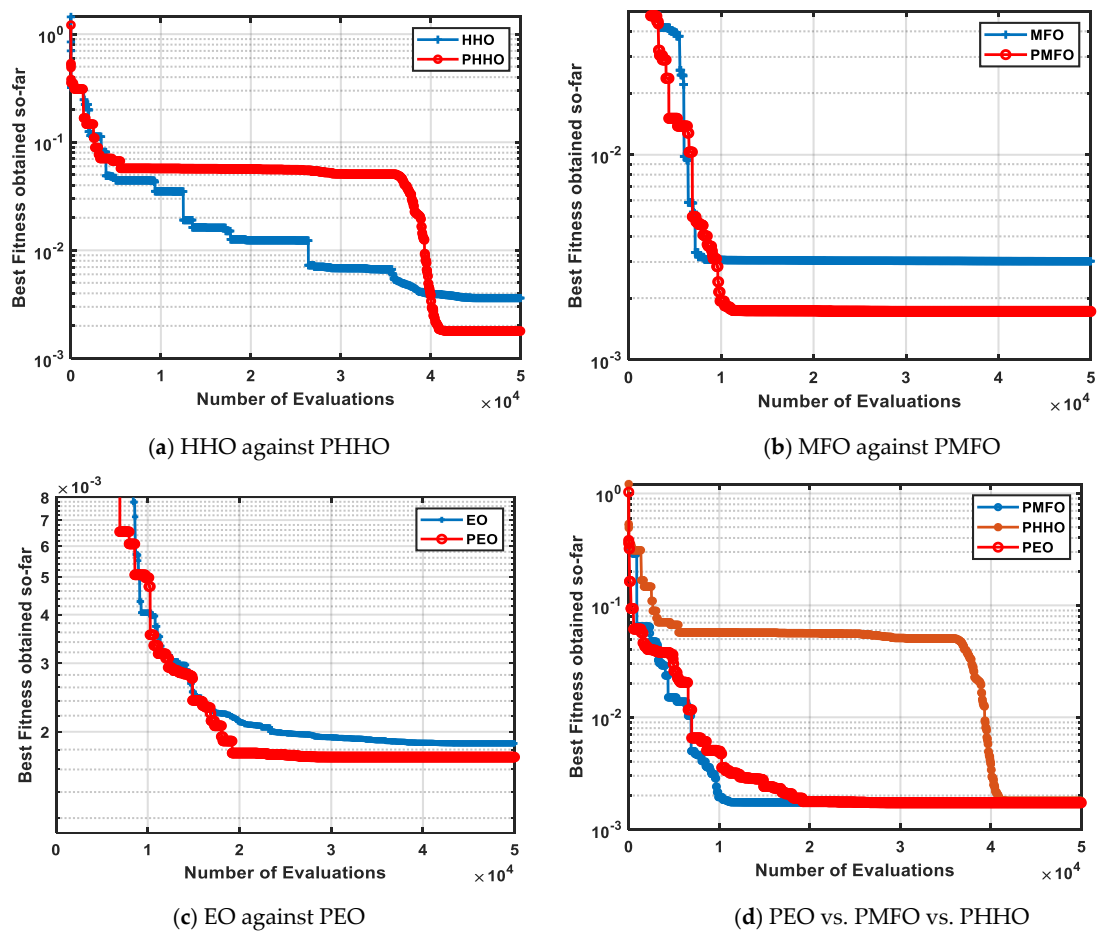
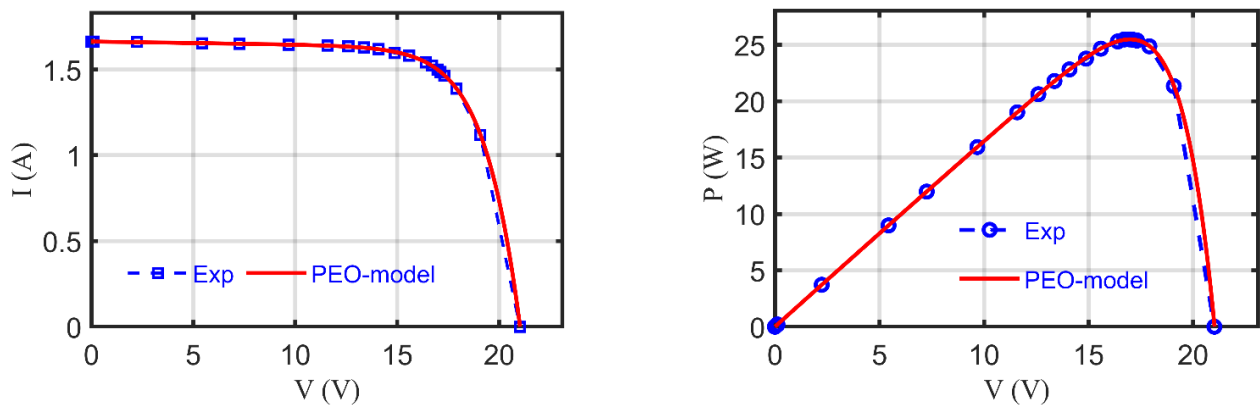


Figure 8. Convergence curves among algorithms in STM6.

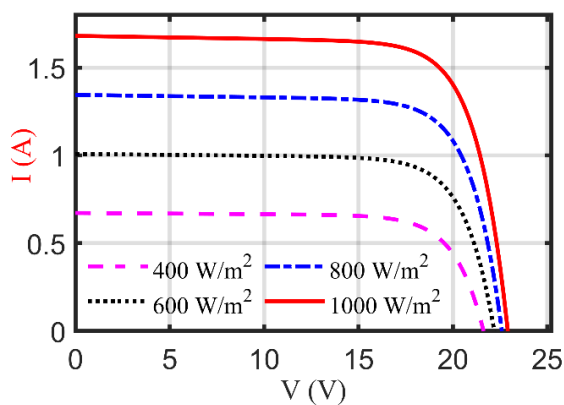
Similar to the abovementioned test cases, many principal characteristics of the STP6-40 module can be produced using the cropped optimal values of the SDM parameters. Figure 9a,b illustrates the I-V and P-V plots of the PEO model against the real/experimental dataset points. On the other hand, various characteristics under varied environmental conditions such as under varied sun irradiances (400–600–800–1000 W/m<sup>2</sup>) are revealed in Figure 9c,d, and under changeable cell, temperatures are shown in Figure 9e,f for 4 levels of temperatures at 0 °C to 75 °C in a step of 25 °C.



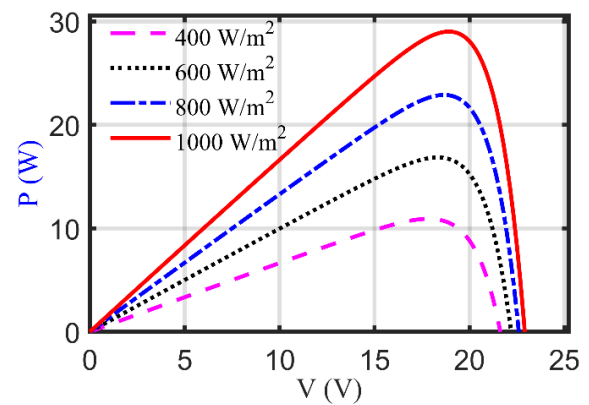
(a) I-V plots of experimental versus PEO model

(b) P-V plots of experimental versus PEO model

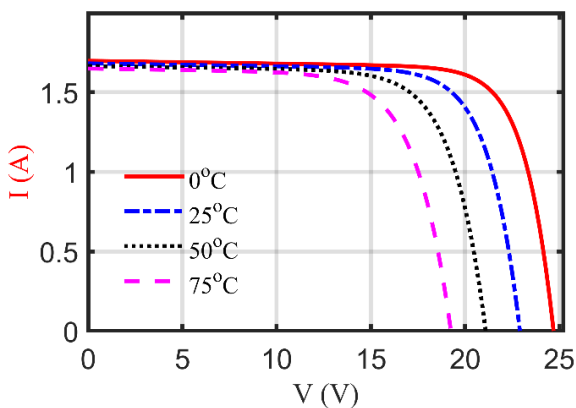
Figure 9. Cont.



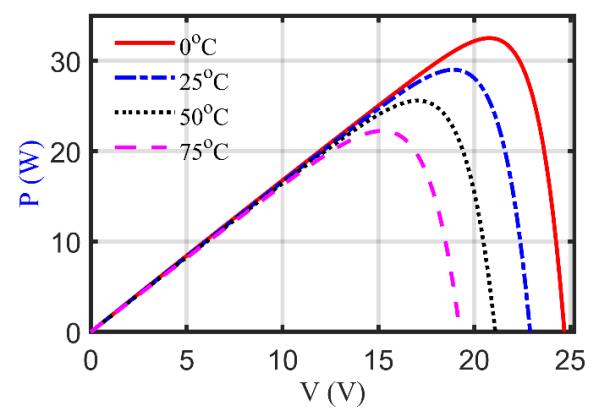
(c) I–V characteristics under different radiation levels



(d) P–V characteristics under different radiation levels



(e) I–V characteristics under varied temperatures



(f) P–V characteristics under varied temperatures

**Figure 9.** Principal characteristics of STM6-40/36PV module.

#### 4.6. Ultra 85-P Module

In this section, a new commercial module, called the Ultra 85-P module, was used to check the performance of the algorithms. The typical nameplate of this module is shown in [46], where it consists of 36 PV cells connected in series and could generate a maximum power of 85 W at standard conditions. This module has an efficiency of 13.4% and 70.3% as a fill factor. To check the performance of the algorithms under this module, Each algorithm was executed 30 independent times and the optimal parameter values and the corresponding RMSE obtained through those runs are presented in Table 9, which show that PEO could reach a value of 0.002551066 for RMSE as the lowest one over the others. Furthermore, Table 10 shows the statistical measures for the best, SD, Avg, and worst obtained in those independent runs. This table confirms the superiority of PEO over the standard and the other algorithms, but unfortunately, both PHHO and PMFO could not exceed the standard ones. In general, our experiments turn out that PCM could significantly improve the performance of the standard EO, and this affirms its efficiency when integrating with some algorithms as an aiding tool to explore some regions, which are intractable by those standard ones. Figure 10a shows the better convergence of PEO, compared to the others. Figure 10b,c illustrates the P–V and I–V plots of the PEO model versus the real/experimental dataset points.

**Table 9.** Comparison under the extracted parameters and the corresponding RMSE of Ultra 85-P.

Algorithms	$I_{ph}(A)$	$I_d(A)$	$R_s(\Omega)$	$R_{sh}(\Omega)$	$n$	RMSE
MFO [39]	5.25403	$2.231 \times 10^{-6}$	0.01243	2.47270	1.40501	0.011839298
PMFO	5.72250	$1.699 \times 10^{-7}$	0.24745	99.9887	1.36073	0.123151236
HHO [38]	5.19832	$2.763 \times 10^{-5}$	0.01009	8.47694	1.69210	0.009073968
PHHO	5.23042	$2.416 \times 10^{-5}$	0.01010	4.36882	1.67431	0.009076382
EO [40]	5.21872	$1.292 \times 10^{-5}$	0.01085	4.41749	1.59388	0.003321018
PEO	<b>5.22707</b>	<b><math>1.043 \times 10^{-5}</math></b>	<b>0.01104</b>	<b>3.79972</b>	<b>1.56822</b>	<b>0.002551066</b>

Bold results are the best option.

**Table 10.** Comparison of statistical measures of STM6.

Algorithms	Best	Worst	Avg	SD	Rank
MFO [39]	0.0118392984	0.1632719909	0.1277740213	0.0233529537	5
PMFO	0.1231512363	0.1789639216	0.1433882756	0.0138564962	6
HHO [38]	0.0090739683	0.2007333708	0.0778740255	0.0680914550	2
PHHO	0.0090763822	0.2453138581	0.0965394055	0.0688037707	3
EO [40]	0.0033210180	0.1234649919	0.0968028058	0.0486708186	4
PEO	<b>0.0025510660</b>	<b>0.1231483292</b>	<b>0.0749094239</b>	<b>0.0600903456</b>	<b>1</b>

Bold results are the best option.

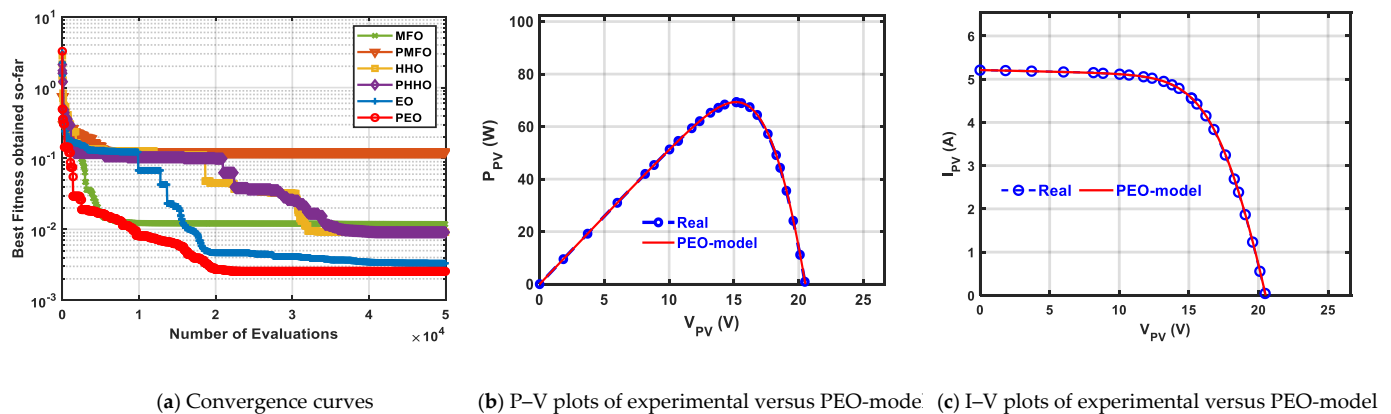


**Figure 10.** Graphical depictions of the performance of the algorithm in Ultra 85-P.

#### 4.7. Comparison of the Studied Algorithms Using Boxplot

In Figure 11, the studied algorithms are compared by drawing the boxplot of THE PWP201, and STM6 modules, and the RTC France solar cell. After running each algorithm for 30 independent runs and depicting the obtained outcomes for those PV modules in Figure 11, it is obvious that the improved algorithms, i.e., PHHO, PEO, and PMFO, outperform their standard versions in all cases. On the other hand, PEO is considered the best option in comparison to all improved variants using PCM, and this shows that hybridization between the classical EO and this method manages to build a new variant having a high ability for widely effective exploration of the search space to reach better outcomes in less number of function evaluations, compared to the classical one.

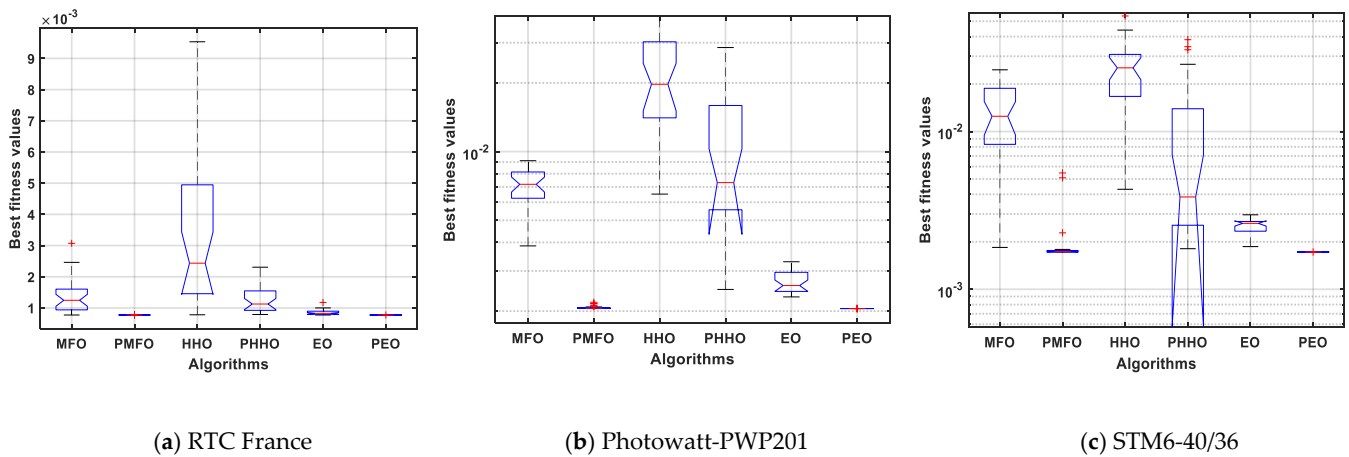


Figure 11. Comparison among algorithms based on Boxplot.

4.8. Wilcoxon Rank-Sum Test

The results obtained within 30 independent runs of each algorithm (original and improved) were compared using the Wilcoxon rank-sum test [47] at a confidence level of 5%. In Table 11, the p-value illustrates the extent of differences in the outcomes obtained by each pair of the algorithms; the h includes only two values: 0 indicates when there is no difference between the outcomes of a pair of the algorithms, and 1 when there is a difference. According to Table 11, for RTC France, the p-value obtained is less than 0.05 for all the improved algorithms against the standard versions, which confirms that there is a difference between the outcomes obtained by each pair of those algorithms. Based on this statistical test and the statistical analysis given in the previous subsections, the improved versions can be accepted as the best option in a significant number of the studied cases. In the same context, Table 12 which compares the difference between the outcomes of PEO as the best-improved variant and all the others under the Wilcoxon rank-sum test, confirms that PEO is the best since it could obtain outcomes significantly different from those of the others.

Table 11. Comparison between the proposed with the others under the Mann–Whitney U test.

Algorithms	RTC		PWP201		STM6	
	h	p-Value	h	p-Value	h	p-Value
MFO vs. PMFO	1	$1.114256 \times 10^{-3}$	1	$2.904721 \times 10^{-1}$	1	$4.615910 \times 10^{-10}$
HHO vs. PHHO	1	$6.843226 \times 10^{-4}$	1	$7.012659 \times 10^{-2}$	1	$2.126464 \times 10^{-4}$
EO vs. PEO	1	$3.017967 \times 10^{-11}$	1	$3.010407 \times 10^{-11}$	1	$3.006634 \times 10^{-11}$

Table 12. Comparison between PEO with the others under the Mann–Whitney U test.

Algorithms	RTC		PWP201		STM6		Ultra 85-P	
	h	p-Value	h	p-Value	h	p-Value	h	p-Value
MFO	1	$3.019859 \times 10^{-11}$	1	$3.019859 \times 10^{-11}$	1	$3.014185 \times 10^{-11}$	1	$1.76972 \times 10^{-10}$
PMFO	1	$3.019859 \times 10^{-11}$	1	$3.338389 \times 10^{-11}$	1	$3.014185 \times 10^{-11}$	1	$3.00663 \times 10^{-11}$
HHO	1	$3.019859 \times 10^{-11}$	1	$3.019859 \times 10^{-11}$	1	$3.014185 \times 10^{-11}$	1	$3.38569 \times 10^{-2}$
PHHO	1	$3.019859 \times 10^{-11}$	1	$3.019859 \times 10^{-11}$	1	$3.014185 \times 10^{-11}$	1	$7.95291 \times 10^{-3}$
EO	1	$3.019859 \times 10^{-11}$	1	$3.019859 \times 10^{-11}$	1	$3.014185 \times 10^{-11}$	1	$1.72503 \times 10^{-6}$

## 5. Conclusions

This paper proposes a new strategy known as the premature convergence method (PCM) in order to accelerate the convergence speed of meta-heuristic algorithms while improving the final accuracy of the optimization algorithms. PCM updates the current individual around the best-so-far solution based on two-step sizes: the first is based on the distance between two individuals selected randomly from the population, while the second is based on the distance between the current solution and the best-so-far solution. For the trade-off between those two steps, a weight variable is used to determine the length of each step size that was added to the best-so-far solution. This weight variable is generated randomly between 0 and 1. Additionally, when the value in this variable is greater than 0.5, emphasis is placed on the second step, and this will increase the exploitation operator of the optimization algorithm. However, if the value of this variable is small, then the exploration capability will be encouraged.

The proposed PCM was integrated with three well-known optimization algorithms—HHO, MFO, and EO—to observe its effectiveness in improving those algorithms' ability to find the unidentified parameters of SDM. After investigating the performance of the improved optimizers on the SDM and PV module model, it is obvious that PCM has a significant effect on the performance of the optimization algorithms, especially EO, for observed cases. The numerical findings obtained by PEO for the observed cases represented in RTC France, PWP201 module, Ultra 85-P, and STM6 module, respectively, are 0.0007730063, 0.0020529606, 0.0025510660, and 0.0017219215. Future work includes improving the control factor of this method to balance exploration and exploitation capability. In addition, we will investigate the performance of PCM with other algorithms that have a balance between the exploration and exploitation at the beginning of the optimization process to investigate if it could improve their performance.

**Author Contributions:** Conceptualization, M.A.-B., R.M., A.E.-F. and M.A.; methodology, M.A.-B., R.M. and M.A.; software, M.A.-B., R.M., M.A. and A.E.-F.; validation, M.A., A.E.-F.; formal analysis, M.A.-B., R.M. and M.A.; investigation, Y.N., A.E.-F. and M.A.; resources, M.A.-B., M.A. and R.M.; data curation, M.A.-B., A.E.-F., R.M. and M.A.; writing—original draft preparation, M.A.-B., R.M. and M.A.; writing—review and editing, Y.N., A.E.-F. and M.A.; visualization, M.A.-B., M.A., A.E.-F. and R.M.; supervision, M.A.-B., M.A. and A.E.-F.; project administration, M.A.-B., R.M. and M.A.; funding acquisition, Y.N. All authors have read and agreed to the published version of the manuscript.

**Funding:** This work was supported by the Soonchunhyang University Research Fund.

**Institutional Review Board Statement:** The study did not involve humans or animals.

**Conflicts of Interest:** The authors declare no conflict of interest.

## References

1. Ayala, H.V.H.; Coelho, L.D.S.; Mariani, V.C.; Askarzadeh, A. An improved free search differential evolution algorithm: A case study on parameters identification of one diode equivalent circuit of a solar cell module. *Energy* **2015**, *93*, 1515–1522. [[CrossRef](#)]
2. Oliva, D.; Cuevas, E.; Pajares, G. Parameter identification of solar cells using artificial bee colony optimization. *Energy* **2014**, *72*, 93–102. [[CrossRef](#)]
3. Awadallah, M.A. Variations of the bacterial foraging algorithm for the extraction of PV module parameters from nameplate data. *Energy Convers. Manag.* **2016**, *113*, 312–320. [[CrossRef](#)]
4. AlHajri, M.; El-Naggar, K.; AlRashidi, M.; Al-Othman, A. Optimal extraction of solar cell parameters using pattern search. *Renew. Energy* **2012**, *44*, 238–245. [[CrossRef](#)]
5. Yeh, W.; Huang, C.; Lin, P.; Chen, Z.; Jiang, Y.; Sun, B. Simplex simplified swarm optimisation for the efficient optimisation of parameter identification for solar cell models. *IET Renew. Power Gener.* **2017**, *12*, 45–51. [[CrossRef](#)]
6. Kiani, A.T.; Nadeem, M.F.; Ahmed, A.; Khan, I.; Elavarasan, R.M.; Das, N. Optimal PV Parameter Estimation via Double Exponential Function-Based Dynamic Inertia Weight Particle Swarm Optimization. *Energies* **2020**, *13*, 4037. [[CrossRef](#)]
7. Li, G.; Chen, X.; Jin, Y. Analysis of the Primary Constraint Conditions of an Efficient Photovoltaic-Thermoelectric Hybrid System. *Energies* **2016**, *10*, 20. [[CrossRef](#)]
8. Ullah, I.; Rasul, M.G. Recent Developments in Solar Thermal Desalination Technologies: A Review. *Energies* **2018**, *12*, 119. [[CrossRef](#)]



9. Jelle, B.P. Building Integrated Photovoltaics: A Concise Description of the Current State of the Art and Possible Research Pathways. *Energies* **2015**, *9*, 21. [\[CrossRef\]](#)
10. Long, W.; Cai, S.; Jiao, J.; Xu, M.; Wu, T. A new hybrid algorithm based on grey wolf optimizer and cuckoo search for parameter extraction of solar photovoltaic models. *Energy Convers. Manag.* **2020**, *203*, 112243. [\[CrossRef\]](#)
11. Liang, J.; Ge, S.; Qu, B.; Yu, K.; Liu, F.; Yang, H.; Wei, P.; Li, Z. Classified perturbation mutation based particle swarm optimization algorithm for parameters extraction of photovoltaic models. *Energy Convers. Manag.* **2020**, *203*, 112138. [\[CrossRef\]](#)
12. Li, S.; Gu, Q.; Gong, W.; Ning, B. An enhanced adaptive differential evolution algorithm for parameter extraction of photovoltaic models. *Energy Convers. Manag.* **2020**, *205*. [\[CrossRef\]](#)
13. Chen, X.; Xu, B.; Mei, C.; Ding, Y.; Li, K. Teaching–learning–based artificial bee colony for solar photovoltaic parameter estimation. *Appl. Energy* **2018**, *212*, 1578–1588. [\[CrossRef\]](#)
14. Ortiz-Conde, A.; Garcia-Sanchez, F.; Muci, J. New method to extract the model parameters of solar cells from the explicit analytic solutions of their illuminated I–V characteristics. *Sol. Energy Mater. Sol. Cells* **2006**, *90*, 352–361. [\[CrossRef\]](#)
15. Tong, N.T.; Kamolpattana, K.; Pora, W. A deterministic method for searching the maximum power point of a PV panel. In Proceedings of the 2015 12th International Conference on Electrical Engineering/Electronics, Computer, Telecommunications and Information Technology (ECTI-CON), Hua Hin, Thailand, 24–27 June 2015.
16. Yu, K.; Liang, J.; Qu, B.; Chen, X.; Wang, H. Parameters identification of photovoltaic models using an improved JAYA optimization algorithm. *Energy Convers. Manag.* **2017**, *150*, 742–753. [\[CrossRef\]](#)
17. Allaoui, M.; Ahiod, B.; El Yafrani, M. A hybrid crow search algorithm for solving the DNA fragment assembly problem. *Expert Syst. Appl.* **2018**, *102*, 44–56. [\[CrossRef\]](#)
18. Abdel-Basset, M.; Mohamed, R.; Elhoseny, M.; Bashir, A.K.; Jolfaei, A.; Kumar, N. Energy-Aware Marine Predators Algorithm for Task Scheduling in IoT-based Fog Computing Applications. *IEEE Trans. Ind. Inform.* **2020**, *17*, 5068–5076. [\[CrossRef\]](#)
19. Abdel-Basset, M.; Chang, V.; Mohamed, R. HSMA\_WOA: A hybrid novel Slime mould algorithm with whale optimization algorithm for tackling the image segmentation problem of chest X-ray images. *Appl. Soft Comput.* **2020**, *95*, 106642. [\[CrossRef\]](#)
20. Zhou, Y.; Yen, G.G.; Yi, Z. A Knee-Guided Evolutionary Algorithm for Compressing Deep Neural Networks. *IEEE Trans. Cybern.* **2019**, *51*, 1626–1638. [\[CrossRef\]](#)
21. Zhang, J.; Zhang, T.; Shin, H.-S.; Wang, J.; Zhang, C. Geomagnetic Gradient-Assisted Evolutionary Algorithm for Long-Range Underwater Navigation. *IEEE Trans. Instrum. Meas.* **2021**, *70*, 2503212. [\[CrossRef\]](#)
22. Xiao, D.; Prado, J.C.D.; Qiao, W. Optimal joint demand and virtual bidding for a strategic retailer in the short-term electricity market. *Electr. Power Syst. Res.* **2021**, *190*, 106855. [\[CrossRef\]](#)
23. Xiao, D.; Prado, J.C.d.; Qiao, W. Winner-leading competitive swarm optimizer with dynamic Gaussian mutation for parameter extraction of solar photovoltaic models. *Electr. Power Syst. Res.* **2021**, *190*, 106855. [\[CrossRef\]](#)
24. Diab, A.A.Z.; Sultan, H.M.; Do, T.D.; Kamel, O.M.; Mossa, M.A. Coyote Optimization Algorithm for Parameters Estimation of Various Models of Solar Cells and PV Modules. *IEEE Access* **2020**, *8*, 111102–111140. [\[CrossRef\]](#)
25. Ridha, H.M.; Heidari, A.A.; Wang, M.; Chen, H. Boosted mutation-based Harris hawks optimizer for parameters identification of single-diode solar cell models. *Energy Convers. Manag.* **2020**, *209*, 112660. [\[CrossRef\]](#)
26. Long, W.; Wu, T.; Jiao, J.; Tang, M.; Xu, M. Refraction-learning-based whale optimization algorithm for high-dimensional problems and parameter estimation of PV model. *Eng. Appl. Artif. Intell.* **2020**, *89*, 103457. [\[CrossRef\]](#)
27. Abdel-Basset, M.; Mohamed, R.; Mirjalili, S.; Chakraborty, R.K.; Ryan, M.J. Solar photovoltaic parameter estimation using an improved equilibrium optimizer. *Sol. Energy* **2020**, *209*, 694–708. [\[CrossRef\]](#)
28. Ridha, H.M.; Gomes, C.; Hizam, H. Estimation of photovoltaic module model's parameters using an improved electromagnetic-like algorithm. *Neural Comput. Appl.* **2020**, *32*, 12627–12642. [\[CrossRef\]](#)
29. Ram, J.P.; Pillai, D.S.; Rajasekar, N.; Chinnaiyan, V.K. Flower Pollination Based Solar PV Parameter Extraction for Double Diode Model. In *Intelligent Computing Techniques for Smart Energy Systems*; Springer: Berlin/Heidelberg, Germany, 2019; pp. 303–312. [\[CrossRef\]](#)
30. Hassan, K.H.; Rashid, A.T.; Jasim, B.H. Parameters estimation of solar photovoltaic module using camel behavior search algorithm. *Int. J. Electr. Comput. Eng.* **2021**, *11*, 788–793. [\[CrossRef\]](#)
31. Kashafi, H.; Sadegheih, A.; Mostafaeipour, A.; Omran, M.M. Parameter identification of solar cells and fuel cell using improved social spider algorithm. *COMPEL Int. J. Comput. Math. Electr. Electron. Eng.* **2020**, *40*, 142–172. [\[CrossRef\]](#)
32. Sharma, A.; Sharma, A.; Averbukh, M.; Jatelly, V.; Azzopardi, B. An Effective Method for Parameter Estimation of a Solar Cell. *Electronics* **2021**, *10*, 312. [\[CrossRef\]](#)
33. Ye, X.; Liu, W.; Li, H.; Wang, M.; Chi, C.; Liang, G.; Chen, H.; Huang, H. Modified Whale Optimization Algorithm for Solar Cell and PV Module Parameter Identification. *Complexity* **2021**, *2021*, 1–23. [\[CrossRef\]](#)
34. Yang, X.; Gong, W. Opposition-based JAYA with population reduction for parameter estimation of photovoltaic solar cells and modules. *Appl. Soft Comput.* **2021**, *104*, 107218. [\[CrossRef\]](#)
35. Mokeddem, D. Parameter Extraction of Solar Photovoltaic Models Using Enhanced Levy Flight Based Grasshopper Optimization Algorithm. *J. Electr. Eng. Technol.* **2020**, *16*, 171–179. [\[CrossRef\]](#)
36. Ismaeel, A.A.K.; Houssein, E.H.; Oliva, D.; Said, M. Gradient-Based Optimizer for Parameter Extraction in Photovoltaic Models. *IEEE Access* **2021**, *9*, 13403–13416. [\[CrossRef\]](#)



37. Sharma, A.; Saxena, A.; Shekhawat, S.; Kumar, R.; Mathur, A. *Solar Cell Parameter Extraction by Using Harris Hawks Optimization Algorithm*; Springer: Singapore, 2020; pp. 349–379. [[CrossRef](#)]
38. Heidari, A.A.; Mirjalili, S.; Faris, H.; Aljarah, I.; Mafarja, M.; Chen, H. Harris hawks optimization: Algorithm and applications. *Futur. Gener. Comput. Syst.* **2019**, *97*, 849–872. [[CrossRef](#)]
39. Mirjalili, S. Moth-flame optimization algorithm: A novel nature-inspired heuristic paradigm. *Knowl. Based Syst.* **2015**, *89*, 228–249. [[CrossRef](#)]
40. Faramarzi, A.; Heidarinejad, M.; Stephens, B.; Mirjalili, S. Equilibrium optimizer: A novel optimization algorithm. *Knowl. Based Syst.* **2020**, *191*, 105190. [[CrossRef](#)]
41. Tan, Y.T.; Kirschen, D.; Jenkins, N. A Model of PV Generation Suitable for Stability Analysis. *IEEE Trans. Energy Convers.* **2004**, *19*, 748–755. [[CrossRef](#)]
42. Gong, W.; Cai, Z. Parameter extraction of solar cell models using repaired adaptive differential evolution. *Sol. Energy* **2013**, *94*, 209–220. [[CrossRef](#)]
43. Nunes, H.G.G.; Pombo, J.; Mariano, S.; Calado, M.D.R.; de Souza, J.F. A new high performance method for determining the parameters of PV cells and modules based on guaranteed convergence particle swarm optimization. *Appl. Energy* **2018**, *211*, 774–791. [[CrossRef](#)]
44. Easwarakhanthan, T.; Bottin, J.; Bouhouch, I.; Boutrit, C. Nonlinear Minimization Algorithm for Determining the Solar Cell Parameters with Microcomputers. *Int. J. Sol. Energy* **1986**, *4*, 1–12. [[CrossRef](#)]
45. Tong, N.T.; Pora, W. A parameter extraction technique exploiting intrinsic properties of solar cells. *Appl. Energy* **2016**, *176*, 104–115. [[CrossRef](#)]
46. Elkholy, M.M.; El-Hameed, M.A.; El-Fergany, A.A. Artificial ecosystem-based optimiser to electrically characterise PV generating systems under various operating conditions reinforced by experimental validations. *IET Renew. Power Gener.* **2021**, *15*, 701–715. [[CrossRef](#)]
47. Haynes, W. Wilcoxon Rank Sum Test. In *Encyclopedia of Systems Biology*; Springer: New York, NY, USA, 2013; pp. 2354–2355.